J. Math. Biol. 49, 227–271 (2004)
Digital Object Identifier (DOI):
10.1007/s00285-003-0256-0

Mathematical Biology

B.W. Kooi · L.D.J. Kuijper · S.A.L.M. Kooijman

Consequences of symbiosis for food web dynamics

Received: 26 March 2003 / Revised version: 21 July 2003 /
Published online: 2 January 2004 –

Abstract. Basic Lotka-Volterra type models in which mutualism (a type of symbiosis where the two populations benefit both) is taken into account, may give unbounded solutions. We exclude such behaviour using explicit mass balances and study the consequences of symbiosis for the long-term dynamic behaviour of a three species system, two prey and one predator species in the chemostat. We compose a theoretical food web where a predator feeds on two prey species that have a symbiotic relationships. In addition to a species-specific resource, the two prey populations consume the products of the partner population as well. In turn, a common predator forages on these prey populations. The temporal change in the biomass and the nutrient densities in the reactor is described by ordinary differential equations (ODE). Since products are recycled, the dynamics of these abiotic materials must be taken into account as well, and they are described by ODEs in a similar way as the abiotic nutrients. We use numerical bifurcation analysis to assess the long-term dynamic behaviour for varying degrees of symbiosis. Attractors can be equilibria, limit cycles and chaotic attractors depending on the control parameters of the chemostat reactor. These control parameters that can be experimentally manipulated are the nutrient density of the inflow medium and the dilution rate. Bifurcation diagrams for the three species web with a facultative symbiotic association between the two prey populations, are similar to that of a bi-trophic food chain; nutrient enrichment leads to oscillatory behaviour. Predation combined with obligatory symbiotic prey-interactions has a stabilizing effect, that is, there is stable coexistence in a larger part of the parameter space than for a bi-trophic food chain. However, combined with a large growth rate of the predator, the food web can persist only in a relatively small region of the parameter space. Then, two zero-pair bifurcation points are the organizing centers. In each of these points, in addition to a tangent, transcritical and Hopf bifurcation a global heteroclinic bifurcation is emanating. This heteroclinic cycle connects two saddle equilibria where the predator is absent. Under parameter variation the period of the stable limit cycle goes to infinity and the cycle tends to the heteroclinic cycle. At this global bifurcation point this cycle breaks and the boundary of the basin of attraction disappears abruptly because the separatrix disappears together with the cycle. As a result, it becomes possible that a stable two-nutrient–two-prey population system becomes unstable by invasion of a predator and eventually the predator goes extinct together with the two prey populations, that is, the complete food web is destroyed. This is a form of over-exploitation by the predator population of the two symbiotic prey populations. When obligatory symbiotic prey-interactions are modelled with Liebig's minimum law, where growth is limited by the most limiting resource, more complicated types of bifurcations are found. This results from the fact that the Jacobian matrix changes discontinuously with respect to a varying parameter when another resource becomes most limiting.

B.W. Kooi, L.D.J. Kuijper, S.A.L.M. Kooijman: Department of Theoretical Biology, Institute of Ecological Science, Faculty of Earth and Life Sciences, Vrije Universiteit, de Boelelaan 1087, 1081 HV Amsterdam, The Netherlands.

Key words or phrases: Bifurcation analysis – Chemostat – Food web – Invasion – Mutualism – Over-exploitation – Persistence – Symbiosis

1. Introduction

The interactions between populations in a food web are generally more complicated than is assumed in the classical models such as the Lotka-Volterra or the Rosenzweig-MacArthur. In those type of models only direct interactions can occur between populations at the same trophic level (competition) or between those at different levels (predator-prey or omnivory). The real world food web interactions are often also indirect, for instance via products excreted by one population and consumed by the partner population. In this paper we will study the effects of this type of digestive symbiosis, often called mutualism when the partners benefit each other [8,10,47,21,4].

We will consider three populations in a chemostat or continuous culture reactor. Two prey populations, which feed on a nutrient, consume also the products of the partner prey population modelling symbiosis. A predator consumes one (specialist) or both (generalist) prey populations. Here we assess how symbiosis affects the long-term dynamics of these food webs.

The prey and predator populations consume multiple resources. These resources can be *essential* or *non-essential*. When an essential resource is missing the population goes always extinct and when the resource is non-essential the population survives if the resource is available in sufficient amounts to pay maintenance costs and other losses.

We will study the consequences of symbiosis by taking four types of two-resources consumption by the prey populations. For each prey population its nutrient and the product of the partner act as substitutable, supplementary, complementary or minimum resources. Substitutability implies that a deficiency in one of the resources can be compensated by using the other, so both are non-essential. A supplementary resource can only be used in addition to the essential resource. It cannot support organisms by their own. Complementary resources are both essential at the same time, they cannot be substituted by the other. This holds also when Liebig's Law of the Minimum is assumed where each prey population is limited by only one resource at a time.

We will use the term symbiosis, that is "living together", instead of mutualism. This avoids the necessity to define what "beneficial" means for a population in the context of a community including all kinds of trophic interactions, such as predator–prey, immigration, emigration and so on. However, we will use the terms facultative and obligatory in the same way as in the mutualism case. Similar as for mutualistic associations between two species, we distinguish two types of symbiotic interactions. In the case of *facultative symbiotic* interaction the products excreted by the partner are non-essential. For substitutable resources the nutrient of the prey is also non-essential while in the supplementary case it is essential. In the case of *obligate symbiosis* both the nutrient and the products of the partner are essential. Complementary and minimum resources are examples. Hence, two species forming a symbiotic association can have different types of symbiotic interaction, for instance a species with a facultative symbiotic interaction lives together with a species with a obligate one.

We restrict ourselves mainly to symmetric dependences where both prey populations have the same type of multiple resources interactions. We will consider one asymmetric dependence where one prey population is the host consuming supplementary resources and the other the symbiont consuming complementary resources. An example is the symbiotic association between algae and other protoctists, plants or animals. In corals algae grow in the tissues of the polyps. These animals get their carbohydrates from the algae and return ammonia that originates from captured zooplankton. Another example are mycorrhizae which are symbiotic associations between plants and fungi that are ubiquitous in terrestrial ecosystems [16,51]. The fungi colonize roots of most plants and can significantly enhance plants ability to extract nutrients (phosphorus P, nitrogen N, copper Cu and zinc Zn) from the soil while they receive from the plant carbohydrates (carbon C) for energy in return.

The standard model for mutualism is the Lotka-Volterra competition model where the negative competitive interactions between the two populations are turned into positive mutualistic interactions. A problem with this formulation is that it can lead to absurd solutions in which both populations explode to unlimited size, an event ironically referred to as "an orgy of mutual benefaction" [33,40,43].

We use a mass-balance model formulation, which renders unbounded solutions impossible. In addition to the three biomass densities of the populations and the two nutrient densities, the two product densities are state variables. Mass-balance model formulation enables the explicit modelling of the temporal change in the density of excreted products. These product densities are essential state variables, because products of one prey species are food for the partner prey species, and this models symbiosis. The mass-balance modelling approach is common practice in biochemistry and microbiology.

We will see that the extension of the mass-balance nutrients–prey–partner model with the introduction of a predator that consumes one (specialist) or both (generalist) prey species, can lead to limit cycle and chaotic solutions but also destruction of the complete food web upon nutrient enrichment when the effective maximum growth rate of the predator is large. With facultative symbiosis, oscillatory dynamics occur at high nutrient supply similar to what happens in a nutrient–prey–predator food chain. With obligatory symbiosis, a stable two-nutrient–two-prey web can be invaded by a predator in a large region of the parameter space, but in a large portion of this region eventually all populations die out due to over-exploitation.

In order to assess the long-term dynamics, we perform a numerical bifurcation analysis. The parameter values were also used in [29] where we studied the effect of a predator on competition for one nutrient between two prey populations. These values are realistic for a microbial food web in a chemostat reactor. Bifurcation parameters are the control parameter which can be experimentally manipulated, the dilution rate (fraction of the volume replaced per unit of time) and the nutrient densities of the inflow medium.

This paper is structured as follows. After the description of standard models for mutualism, firstly alternative types of trophic interactions where one prey population consumes two resources, are described. Second, in order to model symbiosis, the two prey populations each consume their own nutrient and the products excreted by the partner prey population. The resulting models are studied using bifurcation

analysis by calculating bifurcation diagrams with respect to the control parameters. Third, the model is extended by the introduction of a predator preying on one or both prey populations. Of the resulting dynamic systems a numerical bifurcation analysis is performed. Bifurcation diagrams for the various food web structures under chemostat conditions are presented and discussed. We start with the effect of increasing the maximum growth rate of a specialist predator which consumes only one prey. We continue with a generalist predator preying on the two substitutable prey populations. Four types of symbiosis for the two prey populations are considered. Two facultative and two obligate types of symbiosis.

2. The standard model for mutualism

The dynamics of each population is mathematically described by an ODE for the temporal change of its biomass density. In many textbooks the following two-species Lotka-Volterra competition model is described and analysed

$$\frac{dN_1}{dt} = N_1 r_1\big(1 - \frac{N_1(t)}{K_1} - \frac{\alpha_{12}N_2(t)}{K_1}\big)\,, \tag{1a}$$

$$\frac{dN_2}{dt} = N_2 r_2\big(1 - \frac{\alpha_{21}N_1(t)}{K_2} - \frac{N_2(t)}{K_2}\big)\,, \tag{1b}$$

where N_i is the population size as a state variable and r_i (intrinsic growth), K_i (carrying capacity) and α_{ij} (competition coefficient) are the Lotka-Volterra competition model parameters. The interaction terms with the α's model the negative effect of the growth of the partner population due to competition.

Mutualism is an interaction of two species of organisms that benefits both [9, 44]. In ecological texts, see for instance [42], modelling of mutualism is often done by just rewriting the competition term

$$\frac{dN_1}{dt} = N_1 r_1\big(1 - \frac{N_1(t)}{K_1} + \frac{\alpha_{12}N_2(t)}{K_1}\big)\,, \tag{2a}$$

$$\frac{dN_2}{dt} = N_2 r_2\big(1 + \frac{\alpha_{21}N_1(t)}{K_2} - \frac{N_2(t)}{K_2}\big)\,. \tag{2b}$$

The signs of the interaction coefficients α changed from negative to positive [52]. Hence, there is now a positive effect of the growth of the partner population. When the intrinsic growth rates r_i and the carrying capacities $K_i, i = 1, 2$ are all positive the mutualism is called *facultative*, that is each species can survive without the mutualist. When these parameters are all negative the mutualism is called *obligate*, that is neither species can survive on its own.

Different qualitative long-term dynamic behaviours may occur depending on weak ($\alpha_{12}\alpha_{21} < 1$) or strong ($\alpha_{12}\alpha_{21} > 1$) interaction. If the mutualism is facultative, the system converges to either a stable positive equilibrium or goes to infinity, respectively. If on the other hand the mutualism is obligatory, the positive equilibrium is unstable and, depending on the initial conditions, the system will go either extinct or to infinity when the interaction is weak and it goes always to infinity when strong [33].

Hence, mutualisms should be less likely in real world than other types of trophic interaction [39,47] and references therein. Numerous additions to the basic Lotka-Volterra model have been proposed in the literature to get more realistic long-term dynamic behaviour. Ringel *et al.* (1996) studied a four species generalization of this two-species Lotka-Volterra model. Simulation results indicated that even the slight difference of adding two species can have profound effects on the predictions the two-species model makes. Recently Hernandez and Barradas (2003) took the interaction coefficients α density dependent, that is $\alpha_{12}(N_2)$ and $\alpha_{21}(N_1)$. In particular this functional form are chosen such that the interaction coefficients α_{ij} shift from positive to negative as N_j increases. The chief draw-back of such Lotka-Volterra equations is that they lack biological detail.

3. Mass-balance model formulation

This section presents a simple food web model. The food chain version of this model was already described and analysed in other papers, but here we repeat this presentation for convenience and to introduce our notation introduced in Table 1. The food web consists of two nutrient, two prey populations and a predator population. Let $x_{0j}(t)$, $j = 1, 2$ denote the density of the nutrients at time t. Further, let $x_{1j}(t)$, denote biomass densities of the prey populations and $x_2(t)$ of the predator. When two trophic levels are involved in the definition of a parameter, two indices will be used separated by a comma. For instance, $\mu_{i,j}$ denotes the maximum growth rate of a predator x_j, feeding on the prey x_i. All state-variables use the same currency of for instance carbon biomass.

The governing equations for the two-nutrients–two-prey–predator systems in the chemostat constitute a seven-dimensional autonomous dynamical system

Table 1. Parameters and state variables; t=time, m=biomass, v=volume of the reactor. The first subindex denotes the trophic level, $i = 0$, $j = 1, 2$ nutrient, $i, k = 1$, $j = 1, 2, l = 1, 2$, prey and $k = 2$ predator. Some parameters have double indexes separated by a comma to emphasize that these quantities depend on two trophic levels. When the interaction is between two populations at the same trophic level this interaction is via the products excreted by the population indicated by the first index.

Parameter	Dimension	Units	Interpretation
D	t^{-1}	h^{-1}	Dilution rate
$I_{ij,kl}$	t^{-1}	h^{-1}	Maximum food uptake rate
$k_{ij,kl}$	$\mathrm{m\,v}^{-1}$	$\mathrm{mg\,dm}^{-3}$	Saturation constant
m_{kl}	t^{-1}	h^{-1}	Maintenance rate coefficient
t	t	h	Time
x_0	$\mathrm{m\,v}^{-1}$	$\mathrm{mg\,dm}^{-3}$	Substrate density
x_{ij}	$\mathrm{m\,v}^{-1}$	$\mathrm{mg\,dm}^{-3}$	Biomass density
x_r	$\mathrm{m\,v}^{-1}$	$\mathrm{mg\,dm}^{-3}$	Substrate concentration in reservoir
$\mu_{ij,kl}$	t^{-1}	h^{-1}	Maximum population growth rate

$$\frac{dx_{01}}{dt} = (x_{r1} - x_{01})D - \mathcal{I}_{01,11}x_{11} \ , \qquad \frac{dx_{02}}{dt} = (x_{r2} - x_{02})D - \mathcal{I}_{02,12}x_{12} \ , \tag{3a}$$

$$\frac{dp_{11}}{dt} = \mathcal{P}_{11}x_{11} - Dp_{11} - \mathcal{I}_{11,12}x_{12} \ , \qquad \frac{dp_{12}}{dt} = \mathcal{P}_{12}x_{12} - Dp_{12} - \mathcal{I}_{12,11}x_{11} \ , \tag{3b}$$

$$\frac{dx_{11}}{dt} = \big(\mathcal{M}_{11} - D\big)x_{11} - \mathcal{I}_{11,2}x_2 \ , \qquad \frac{dx_{12}}{dt} = \big(\mathcal{M}_{12} - D\big)x_{12} - \mathcal{I}_{12,2}x_2 \ , \tag{3c}$$

$$\frac{dx_2}{dt} = \big(\mathcal{M}_2 - D\big)x_2 \ . \tag{3d}$$

The material flows are schematically shown in Fig. 1. The reservoir density of the abiotic nutrients in the medium inflow are denoted by $x_{rj} \geq 0$, $j = 1, 2$ and $D \geq 0$ is the dilution rate. The trophic interactions are via ingestion rates denoted by $\mathcal{I}$. The predator x_2 consumes one (specialist) or both (generalist) prey populations. Prey x_{1j} consumes its nutrient x_{0j} and the product $p_{1(3-j)}$ excreted by the partner $x_{1(3-j)}$, $j = 1, 2$. All components are removed from the reactor with a loss rate equal to the dilution rate D.

The ingested food is used for growth $\mathcal{M}$ whereby products with a rate $\mathcal{P}$ are formed and excreted in the reactor. We assume that only one product is formed per species and that all product is a usable resource for the partner. Then the mass

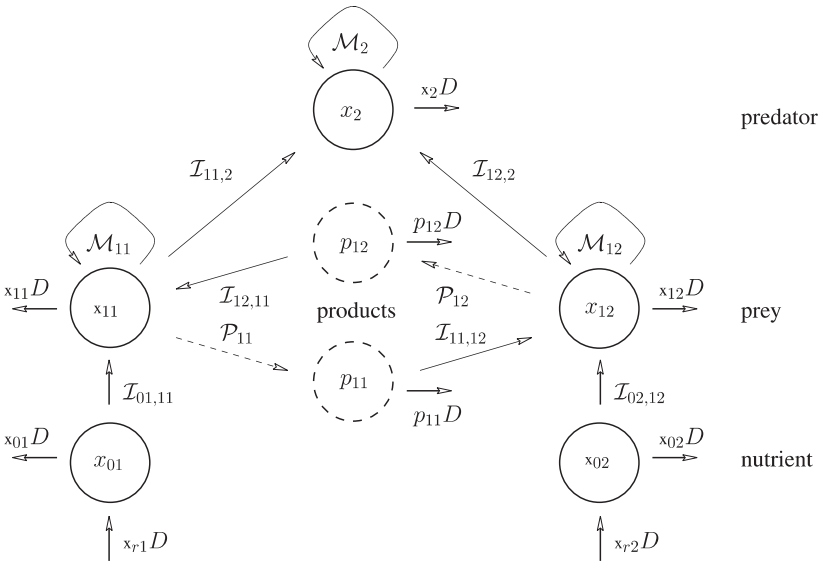

Fig. 1. Material flows through the food web with symbiotic interactions between the two prey populations. The solid arrows indicate ingestion, $\mathcal{I}$. The dashed arrows indicate excretion of products, faeces and respiratory products, $\mathcal{P}$. The growth rates are denoted by $\mathcal{M}$.

conservation law for the material flows through the prey species at the population level, leads directly to

$$\mathcal{P}_{11} = \mathcal{I}_{01,11} + \mathcal{I}_{12,11} - \mathcal{M}_{11} \ , \quad \mathcal{P}_{12} = \mathcal{I}_{02,12} + \mathcal{I}_{11,12} - \mathcal{M}_{12} \ . \tag{4}$$

The growth of the prey populations $\mathcal{M}_{1,j}$ is rate-limited only by the availability of the nutrients $\mathcal{I}_{0j,1j}$ and the products formed by the partner $\mathcal{I}_{1(3-j),1j}$ (see Fig. 1). All the other required nutrients are present in the reactor in excess and are therefore non-limiting. Hence, the product formed by the population is a net product. It is the difference between those products formed and excreted by the population and the non-limiting nutrients ingested in addition to the limiting nutrients.

As an example, we describe the mass-balance model for a bi-trophic food chain in the chemostat where double indices are not necessary

$$\frac{dx_0}{dt} = (x_r - x_0)D - I_{0,1}\frac{x_0}{k_{0,1} + x_0}x_1 \ , \tag{5a}$$

$$\frac{dp_1}{dt} = \big((I_{0,1} - \mu_{0,1})\frac{x_0}{k_{0,1} + x_0} + m_1\big)x_1 - Dp_1 \ , \tag{5b}$$

$$\frac{dx_1}{dt} = \big(\mu_{0,1}\frac{x_0}{k_{0,1} + x_0} - m_1 - D\big)x_1 - I_{1,2}\frac{x_1}{k_{1,2} + x_1}x_2 \ , \tag{5c}$$

$$\frac{dp_2}{dt} = \big((I_{1,2} - \mu_{1,2})\frac{x_1}{k_{1,2} + x_1} + m_2\big)x_2 - Dp_2 \ , \tag{5d}$$

$$\frac{dx_2}{dt} = \big(\mu_{1,2}\frac{x_1}{k_{1,2} + x_1} - m_2 - D\big)x_2 \ . \tag{5e}$$

The maximum growth rate $\mu_{u,i} > 0$ is attained when resource are abundant and no maintenance costs ($m_i = 0$). The quotient of this maximum growth rate and the maximum ingestion rate $I_{u,i} > 0$, $y_{u,i} = \mu_{u,i}/I_{u,i}$ is called (assimilation) efficiency in ecology and yield in microbiology. The yield is positive and generally less than one. It can be greater than one when the nonlimiting nutrients would be consumed at a rate higher than the products are formed. These products include the un-assimilated parts of the resources. Metabolic products are formed with a rate proportional to the maintenance rate coefficient $m_i \geq 0$. Hence, products p_1 and p_2 are each formed by two processes, assimilation (faeces) and maintenance. Biotic x_1, x_2 as well as abiotic x_0, p_1, p_2 components are washed-out with the dilution rate.

In this food chain example, the products excreted by the prey and the predator population are not consumed by one of the species and therefore (5b) and (5d) are decoupled from the other equations of system (5).

When nutrient recycling is subject of investigation, all equations of system (5) are interconnected and the dynamics of the products have to be modelled explicitly. Digestive symbiosis is a type of recycling of products produced by the prey populations and therefore the products formed by the prey populations must be taken into account explicitly.

The classical Holling type II scaled functional response which is used for the nutrient–prey interaction reads

$$f_{u,i}(x_u) = \frac{x_u/k_{u,i}}{1 + x_u/k_{u,i}} \ . \tag{6}$$

We consider this type of trophic interaction as a pseudo-reaction scheme as follows:

$$\mathrm{X^s} + \mathrm{N} \overset{I_{N,X}/k_{N,X}}{\longrightarrow} \mathrm{X^{hN}} \overset{I_{N,X}}{\rightarrow} \mathrm{X^s} \ . \tag{7}$$

In case of the nutrient-prey interaction, N denotes the nutrient and X the prey. The prey can be in two states: $\mathrm{X^s}$ is the searching state, and $\mathrm{X^{hN}}$ the state of handling the nutrient which are supplied in discrete portions (molecules but also particles). The rates associated with mass action terms are the search rate between a prey individual and a nutrient particle, and the return rate from handling. Using time-budgets and time-scale separation the scaled functional response (6) can be found analogous to the predator-prey interaction formulation in ecology (Holling type II) and the enzyme-kinetic (Michaelis–Menten) relationship in biochemistry and microbiology, see [14,41,43]. Although complicated formalisms, similar to multimolecular reaction schemes with indermediate stages (see [14]), can be used, in this paper we consider only simple schemes.

The quasi-steady-state assumption, that is, the fractions of the individuals in the searching and handling state change instantaneously to the stable equilibrium of the fast system, even when the amount of nutrient and/or the biomass of the prey population change (relatively slowly). The search rate equals $I_{N,X}/k_{N,X}$, that is the maximum ingestion rate $I_{N,X}$ divided by the saturation constant $k_{N,X}$. The return rate from handling equals the maximum ingestion rate $I_{N,X}$. Hence $1/I_{N,X}$ is the handling time.

3.1. Multiple resources trophic interactions

When there are two or more limiting resources, it is necessary to consider how the resources are consumed and how they interact to give growth and product formation. Each predator individual encounters now particles from both resources, which can be molecules but also entire prey individuals, and handles these different particles at a different speed.

In the literature, see for example [17,22,38,50], two, or more, resources are classified as *substitutable*, *complementary*, *essential*, *interactive-essential* and *hemi–essential*.

Here, we start with multiple resource consumption using the pseudo-reaction scheme. Applying time-scale arguments yields scaled functional responses which are part of the ingestion $\mathcal{I}$, growth $\mathcal{M}$, and product formation $\mathcal{P}$ rates in the governing equations (3).

Most heterotrophs probably consume resources that are substitutable. Autotrophs require mineral nutrients like carbon, nitrogen, phosphorus and sulfur, which cannot be substituted one for the other. These are examples of multiple resources trophic interactions where both resources are essential (see [17]).

3.1.1. Substitutable resources

The pseudo-reaction scheme, which reflexes the trophic interaction, reads now

$$\mathrm{X^s} + \mathrm{N} \overset{I_{N,X}/k_{N,X}}{\longrightarrow} \mathrm{X^{hN}} \overset{I_{N,X}}{\rightarrow} \mathrm{X^s}\,, \tag{8a}$$

$$\mathrm{X^s} + \mathrm{P} \overset{I_{P,X}/k_{P,X}}{\longrightarrow} \mathrm{X^{hP}} \overset{I_{P,X}}{\rightarrow} \mathrm{X^s}\,. \tag{8b}$$

In this nutrient–partner's product–one-prey interaction formulation, N and P denote the nutrient and products, respectively, and X the prey population. The prey can be in three states: $\mathrm{X^s}$ is the searching state, and $\mathrm{X^{hN}}$ the state of handling nutrient N and $\mathrm{X^{hP}}$ the state of handling products P. The rates $I_{N,X}$, $I_{P,X}$ are the maximum ingestion rates and $k_{N,X}$, $k_{P,X}$ are the saturation constants. A classical time-budget approach leads to the following scaled functional response

$$f^{sub}_{uv,iv}(x_{uv}, p_{iw}) = \frac{x_{uv}/k_{uv,iv}}{1 + x_{uv}/k_{uv,iv} + p_{iw}/k_{iw,iv}}\,, \tag{9a}$$

$$f^{sub}_{iw,iv}(x_{uv}, p_{iw}) = \frac{p_{iw}/k_{iw,iv}}{1 + x_{uv}/k_{uv,iv} + p_{iw}/k_{iw,iv}}\,. \tag{9b}$$

The handling time of a prey for both resources, its nutrient and its partner's products, are assumed to be the same $I_{P,X} = I_{N,X}$, but this is not required here.

3.1.2. Supplementary resources

With supplementary resources the nutrient is assumed to be essential and the product of the partner is non-essential. That is, when its nutrient is missing the prey population goes extinct, but when the non-essential products of the partner are missing, it survives. The scaled functional responses can be derived using the following scheme for this type of trophic interaction

$$\mathrm{X^s} + \mathrm{N} \overset{I_{N,X}/k_{N,X}}{\longrightarrow} \mathrm{X^{hN}} \overset{I_{N,X}}{\rightarrow} \mathrm{X^s}\,, \tag{10a}$$

$$\mathrm{X^{hN}} + \mathrm{P} \overset{I_{P,X}/k_{P,X}}{\longrightarrow} \mathrm{X^{hNP}} \overset{I_{NP,X}}{\rightarrow} \mathrm{X^s}\,. \tag{10b}$$

The handling time of a prey for both resources, its nutrient and its partner's products, is taken the same $I_{P,X} = I_{N,X}$. The handling time of the nutrient-partner's product compound NP is assumed to be zero for sake of simplicity. That is $I_{NP,X} = \infty$ (as in the classical linear Lotka-Volterra functional response being the limiting case of the Holling type II functional response where handling time for the single resource is zero). The following notation is introduced

$$f^{sup}_{uv,iv}(x_{uv}, p_{iw}) = \frac{x_{uv}/k_{uv,iv}(1 + p_{iw}/k_{iw,iv})}{1 + x_{uv}/k_{uv,iv} + p_{iw}/k_{iw,iv}}\,, \tag{11a}$$

$$f^{sup}_{iw,iv}(x_{uv}, p_{iw}) = \frac{x_{uv}/k_{uv,iv}\ p_{iw}/k_{iw,iv}}{1 + x_{uv}/k_{uv,iv} + p_{iw}/k_{iw,iv}}\,, \tag{11b}$$

where $i = u + 1$, $v = 1, 2$ and $w = 3 - v$.

3.1.3. Complementary resources
We assume the following scheme for this type of trophic interaction

$$X^s + N \xrightarrow{I_{N,X}/k_{N,X}} X^{hN} \quad , X^{hP} + N \xrightarrow{I_{N,X}/k_{N,X}} X^{hNP} , \tag{12a}$$

$$X^s + P \xrightarrow{I_{P,X}/k_{P,X}} X^{hP} \quad , X^{hN} + P \xrightarrow{I_{P,X}/k_{P,X}} X^{hNP} , \tag{12b}$$

$$X^{hNP} \xrightarrow{I_{NP,X}} X^s . \tag{12c}$$

The scaled functional responses become

$$f^{com}_{uv,iv}(x_{uv}, p_{iw}) = f^{com}_{iw,iv}(x_{uv}, p_{iw}) = \\ = \frac{x_{uv}/k_{uv,iv}\ p_{iw}/k_{iw,iv}}{x_{uv}/k_{uv,iv} + p_{iw}/k_{iw,iv} - \frac{x_{uv}/k_{uv,iv}\ p_{iw}/k_{iw,iv}}{x_{uv}/k_{uv,iv}+p_{iw}/k_{iw,iv}}} , \tag{13}$$

where $i = u + 1$, $v = 1, 2$ and $w = 3 - v$. This formulation is proposed in [31] to model assimilation and growth, called a Synthesizing Unit. For simplicity we take again $I_{P,X} = I_{N,X}$ and $I_{NP,X} = \infty$, that is no handling time is needed for the NP compound. Notice that the ingestion rates for both nutrients are equal. The resources that obey (13) are of a type called *interactive-essential* in Tilman (1982) while he used the term complementary resources for a different type of multiple resource interaction not discussed here.

3.1.4. Liebig-minimum law
We also consider the Liebig-minimum law multiple resource formulation where it is assumed that each prey is limited by only one resource at a time. There is a considerable literature on competition of multiple prey populations for multiple resources, we mention [17,22,38,50]. Tilman developed a graphical technique to analyse these competition models. There is no quasi-chemical reaction scheme for this formulation. The scaled functional response for the trophic-interaction reads now

$$f^{min}_{uv,iv}(x_{uv}, p_{iw}) = f^{min}_{iw,iv}(x_{uv}, p_{iw}) = \min\Big(\frac{x_{uv}}{k_{uv,iv} + x_{uv}}, \frac{p_{iw}}{k_{iw,iv} + p_{iw}}\Big) , \tag{14}$$

with the same rules for the subindices as given above. We assumed again $I_{P,X} = I_{N,X}$. The minimum is taken over the scaled functional responses as is done in [18], but in most papers the minimum is taken over the scaled functional responses times a maximum ingestion rate which differs for each resource. The resources that obey Liebig's Law are often referred to as *essential* or *perfectly essential* in the literature.

3.2. Symbiotic associations

The various multiple resource trophic interactions described in the previous section can be combined with the formulation of a symbiotic association between two prey populations. In principle all combinations are possible.

We study all symmetric cases where both prey populations have the same multiple resource interactions and we call this substitutable, supplementary, complementary and minimum symbiosis when both consume their nutrients and the products

of the partner are complementary, and so on. The first two types lead to *facultative symbiosis* (for each prey population the products of its partner are non-essential resources) and the two latter types fall under the category of *obligate symbiosis* (for each prey population the products of its partner are essential resources).

One asymmetric case is considered where for a host, its nutrient and the products of the symbiont partner are supplementary, while for a symbiont, its nutrient and products of the host partner are complementary.

We conclude this section with the formulation of the ingestion, growth and product formation rates terms of the governing equations (3) for the various symbiotic interactions between the prey populations. Focusing on terms relating to species 1, Fig. 1 illustrates the meaning of $\mathcal{I}_{01,11}$, $\mathcal{I}_{12,11}$, $\mathcal{M}_{11}$ and $\mathcal{P}_{11}$, and the analogous terms for species 2.

$$\mathcal{I}_{uv,iv} = I_{uv,iv} f_{uv,iv}(x_{uv}, p_{iw}) \ , \tag{15a}$$

$$\mathcal{I}_{iw,iv} = I_{iw,iv} f_{iw,iv}(x_{uv}, p_{iw}) \ , \tag{15b}$$

$$\mathcal{M}_{iv} = \mu_{uv,iv} f_{uv,iv}(x_{uv}, p_{iw}) + \mu_{iw,iv} f_{iw,iv}(x_{uv}, p_{iw}) - m_{iv} \ , \tag{15c}$$

$$\begin{aligned} \mathcal{P}_{iv} = {} & (I_{uv,iv} - \mu_{uv,iv}) f_{uv,iv}(x_{uv}, p_{iw}) \\ & + (I_{iw,iv} - \mu_{iw,iv}) f_{iw,iv}(x_{uv}, p_{iw}) + m_{iv} \ , \end{aligned} \tag{15d}$$

where again $u = 0$, $v = 1, 2$ and $i = u + 1$, $w = 3 - v$ and $f_{uv,iv} = f^{sub}_{uv,iv}$, $f_{iw,iv} = f^{sub}_{iw,iv}$: (9) for the substitutable, $f_{uv,iv} = f^{sup}_{uv,iv}$, $f_{iw,iv} = f^{sup}_{iw,iv}$: (11) for the supplementary, $f_{uv,iv} = f^{com}_{uv,iv}$, $f_{iw,iv} = f^{com}_{iw,iv}$: (13) for the complementary and finally $f_{uv,iv} = f^{min}_{uv,iv}$, $f_{iw,iv} = f^{min}_{iw,iv}$: (14) for the Liebig-minimum law case. We assume $I_{01,11} = I_{12,11}$ and $I_{02,12} = I_{11,12}$, but the saturation constants $k_{01,11}$, $k_{12,11}$, $k_{01,11}$, $k_{12,11}$ differ, see Table 3. So, for each prey species the handling times are equal but the search rates differ. In Table 2 the growth rates for the four types

Table 2. List of limiting growth rates of prey population x_{11} consuming both its nutrient x_{01} and products of its partner p_{12}. Resources can be essential or non-essential for a population to survive. In the case of multiple resources each resource can be essential or non-essential. For facultative symbiosis between both populations the product excreted by the partner are non-essential resources while for obligate symbiosis they are essential resources.

Symbiosis	Growth rate
Facultative	
substitutable	$\frac{\mu_{01,11} x_{01}/k_{01,11} + \mu_{02,11} p_{12}/k_{12,11}}{1 + x_{01}/k_{01,11} + p_{12}/k_{12,11}}$
supplementary	$\frac{\mu_{01,11} x_{01}/k_{01,11}(1 + p_{12}/k_{12,11}) + \mu_{02,11} x_{01} p_{12}/k_{12,11}}{1 + x_{01}/k_{01,11} + p_{12}/k_{12,11}}$
additive	$\mu_{01,11} \frac{x_{01}}{k_{01,11} + x_{01}} + \mu_{02,11} \frac{p_{12}}{k_{12,11} + p_{12}}$
Obligatory	
complementary	$\frac{\mu_{01,11} x_{01}/k_{01,11}\, p_{12}/k_{12,11}}{x_{01}/k_{01,11} + p_{12}/k_{12,11} - (x_{01}/k_{01,11}\, p_{12}/k_{12,11})/(x_{01}/k_{01,11} + p_{12}/k_{12,11})}$
minimum	$\mu_{01,11} \min\left(\frac{x_{01}}{k_{01,11} + x_{01}}, \frac{p_{12}}{k_{12,11} + p_{12}}\right)$
multiplicative	$\mu_{01,11}\left(\frac{x_{01}}{k_{01,11} + x_{01}} \times \frac{p_{12}}{k_{12,11} + p_{12}}\right)$

Table 3. Parameter set for bacterium-ciliate model, after Cunningham and Nisbet (1983). These values were also used in [29]. The ranges for the control parameters are $0 < D < \mu_{0,11}$ and $0 < x_r \leq 300$ mg dm^{-3}.

Parameter	Unit	Values					
		$i=0$ $j=1$	$i=1$ $j=1$	$i=1$ $j=2$	$i=0$ $j=2$	$i=1$ $j=1$	$i=1$ $j=2$
		$k=1$				$k=2$	
		$l=1$	$l=2$	$l=1$	$l=2$		
$\mu_{ij,kl}$	h^{-1}	0.5	0.42	0.5	0.42	0.2	0.3
$I_{ij,kl}$	h^{-1}	1.25	1.05	1.25	1.05	0.33	0.33
$k_{ij,kl}$	mg dm^{-3}	8	11	16	5.5	9	9.1
m_{kl}	h^{-1}	0.025				0.01	

of symbiotic association are summarized. The $\mu_{uv,iv}$'s are the maximum growth rates where the prey consumes solely its essential nutrient.

In Fig. 2 the growth isoclines for two substitutable (a) and two supplementary (b) resources are depicted. Observe that x_{01} has to be positive in order to get a positive growth rate of the prey x_{11}. For low non-essential resource density p_{12} and rather high essential nutrient density x_{01} the growth rate in the supplementary case is larger than for substitutable resources and for low essential resource density it is just the reverse. Figure 2(c) gives the isoclines for complementary resources. The growth isoclines for minimum resources Fig. 2(d) are rectilinear. For moderate growth rates the isoclines in the case of two complementary resources resembles those for the two minimum resources.

4. Bifurcation analysis of symbiosis model

We introduce the total nutrient density in the inflow $x_r = x_{r1} + x_{r2}$ and a mixing factor ρ, by $x_{r1} = \rho x_r$ and $x_{r2} = (1-\rho)x_r$. This makes it possible to use x_r and ρ besides D as bifurcation parameters. In order to perform a numerical bifurcation analysis we have to make choices for the parameter values. We use the species parameter set for bacterium-ciliate models, taken from Cunningham and Nisbet (1983) and given in Table 3.

The bifurcation diagrams were calculated with the computer programs AUTO [13] and LOCBIF [25] or CONTENT [36]. The Liebig-minimum law case deserves some special attention. Under parameter variation the Jacobian matrix evaluated at an equilibrium will generally be discontinuous with respect to that parameter at the point another resource becomes most limiting. This hampers the usage of bifurcation packages mentioned. These packages can be used straightforwardly on branches where no change of the most limiting resource takes place. We used a computer program provided by Boer (2000) to continue the switching points. In Table 4 the notation for the different type of attractors are introduced and Table 5 gives a list of all bifurcation curves.

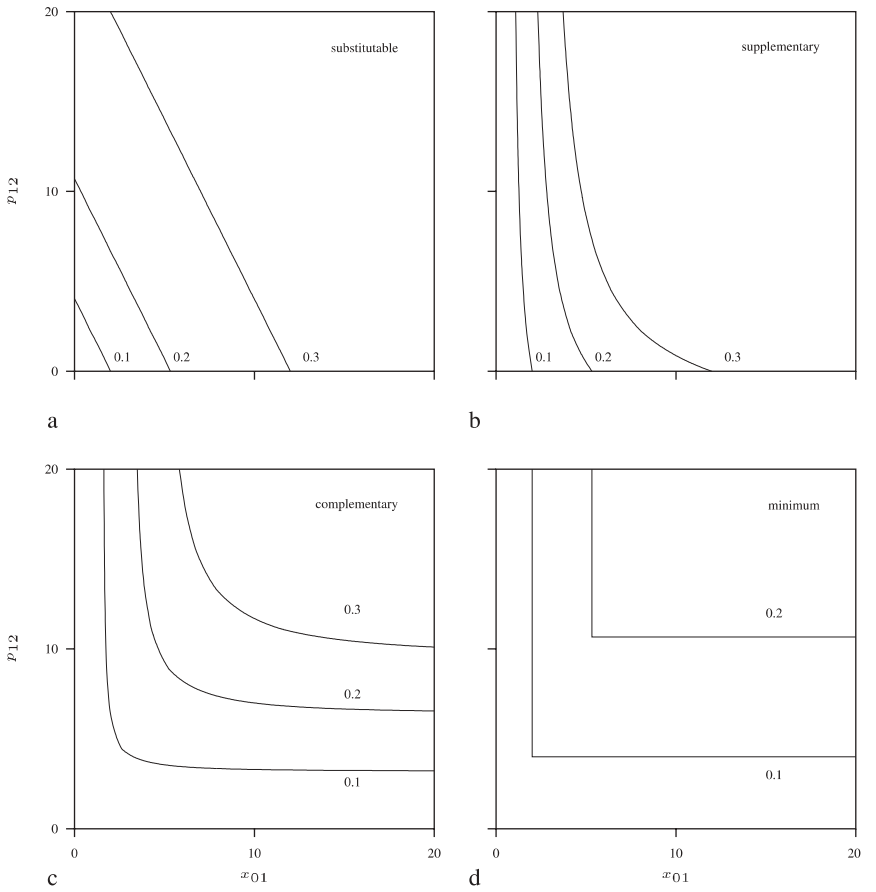

Fig. 2. Growth isoclines for prey population x_{11} feeding on its nutrient x_{01} and the products of its partner p_{12}. **a**: substitutable, **b**: supplementary, **c**: complementary and **d**: minimum resources. Parameter values are: $\mu_{01,11} = 0.5$, $\mu_{12,11} = 0.5$ and $k_{01,11} = 8$, $k_{12,11} = 16$.

In Fig. 3 the biomasses of the two prey populations are depicted in one-parameter diagrams where the total density of the incoming nutrients, x_r is the bifurcation parameter, with $\rho = 0.5$ and $D = 0.1$. In this one-parameter bifurcation diagram for substitutable symbiosis, Fig. 3(a), and supplementary symbiosis, Fig. 3(b), there are two transcritical bifurcations denoted by TC_{12} and $TC_{12,11}$. For x_r values below TC_{12} the zero solution, $E_{01,02}$ is stable and no prey can invade. Between the curves TC_{12} and $TC_{12,11}$, the equilibrium point E_{12} is stable and above $TC_{12,11}$ the stable equilibrium point $E_{11,12}$ is the single attractor.

In the two-parameter bifurcation diagrams x_r and ρ are the free parameters. The two two-parameter bifurcation diagrams differ a lot for values of ρ close to zero and one, that is only one substrate is supplied. With substitutable symbiosis, Fig. 3(c), the two prey populations can live on one single nutrient. This follows from the fact that the transcritical curves $TC_{11,12}$ and $TC_{12,11}$ intersect the $\rho = 0$ and $\rho = 1$

Table 4. Equilibria and limit cycles attractors of the nutrient-prey-partner (Fig. 6(a)), nutrient-prey-partner-predator (Fig. 6(c,d)) food web and the food web without symbiosis (Fig. 6(b)). With symbiotic interactions together with the prey populations x_{11} and x_{12}, the products p_{11} and p_{12} exist but they are not indicated. The attractor is an equilibrium A = E or a limit cycle A = L.

Trophic levels	Equilibrium
nutrient	$A_{01} = (x_{01}, 0, 0, 0, 0)$
nutrients	$A_{01,02} = (x_{01}, x_{02}, 0, 0, 0)$
nutrient-prey	$A_{01,11} = (x_{01}, 0, x_{11}, 0, 0)$
nutrient-partner	$A_{02,12} = (0, x_{02}, 0, x_{12}, 0)$
nutrients-prey	$A_{11} = (x_{01}, x_{02}, x_{11}, 0, 0)$
nutrients-partner	$A_{12} = (x_{01}, x_{02}, 0, x_{12}, 0)$
nutrients-prey-partner	$A_{11,12} = (x_{01}, x_{02}, x_{11}, x_{12}, 0)$
nutrient-prey-predator	$A_{01,11,2} = (x_{01}, 0, x_{11}, 0, x_2)$
nutrients-prey-predator	$A_{11,2} = (x_{01}, x_{02}, x_{11}, 0, x_2)$
nutrients-partner-predator	$A_{12,2} = (x_{01}, x_{02}, 0, x_{12}, x_2)$
nutrients-prey-partner-predator	$A_{11,12,2} = (x_{01}, x_{02}, x_{11}, x_{12}, x_2)$

Table 5. List of the bifurcations curves and points.

Bifurcation	Description
	Bifurcation curves
TC_{2j}	Transcritical bifurcation: invasion through boundary equilibrium by prey (x_{1j}) into the nutrient (x_{0j}) system
$TC_{1i,1j}$	Transcritical bifurcation: invasion through boundary equilibrium by prey (x_{1j}) into the nutrient–prey, (x_{0i},x_{1i}) system
TC_3	Transcritical bifurcation: invasion through boundary equilibrium by predator into nutrients–two-prey system
$T_{1i,1j}$, $Q_{1i,1j}$	tangent and pseudo-tangent bifurcation for prey x_{1i} and x_{1j}, disappearance of two equilibria
$Q^+_{1,2}$, $Q^-_{1,2}$	pseudo-tangent, pseudo-Hopf bifurcation, collapse of complete food web and origin of limit cycle
H^-_{2j}	supercritical Hopf bifurcation of nutrient–prey–predator (x_{0j},x_{1j},x_2) system, food web becomes unstable and origin of stable limit cycle
H^-_3	supercritical Hopf bifurcation of nutrients–two-prey–predator system: food web becomes unstable and origin of stable limit cycle
	Codim-2 points
O	Transcritical–tangent bifurcation point
P	zero-pair point
	Global bifurcation curves
$G^{\neq}_e$	Heteroclinic loop, connections between two saddle points, collapse of complete food web
$G^{=}_e$	Homoclinic Shil'nikov bifurcation, 'skeleton' for chaotic dynamics
$G^{=}_c$	Homoclinic loop for limit cycle, collapse of predator

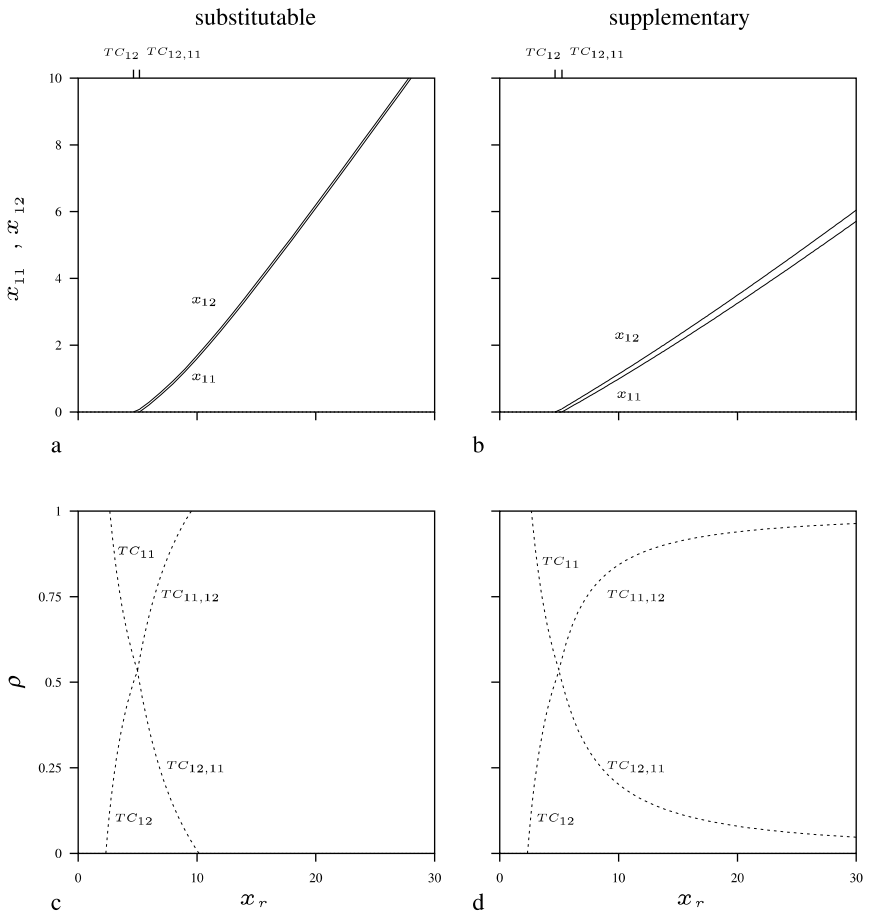

Fig. 3. Bifurcation diagrams with facultative symbiosis between two prey without the predator (Fig. 6(a)): One-parameter diagrams for substitutable (**a**) and supplementary (**b**) symbiosis for equilibrium values of the prey x_{11} and x_{12}. The bifurcation parameter is the concentration in the reservoir is x_r where $\rho = 0.5$. The dilution rate is $D = 0.1$. Two-parameter bifurcation diagrams for substitutable (**c**) and supplementary (**d**) symbiosis where the bifurcation parameters are the concentration in the reservoir is x_r and the mixing factor ρ. The dilution rate is $D = 0.1$.

lines respectively. This does not hold for the supplementary symbiosis, Fig. 3(d), there these two curves bend to infinity approaching the $\rho = 0$ or $\rho = 1$ line.

Fig. 4 gives the results for obligate symbiosis. For complementary symbiosis there is a tangent bifurcation denoted by $T_{11,12}$, instead of a transcritical bifurcation. This tangent bifurcation forms the boundary of the region in the parameter space where two positive equilibria coexists besides a zero equilibrium $E_{01,02}$. This zero equilibrium is now always stable while one of the positive equilibria is stable and the other unstable. There is some kind of dead-lock. One prey population needs the products of the second prey while at the same time the second one needs the

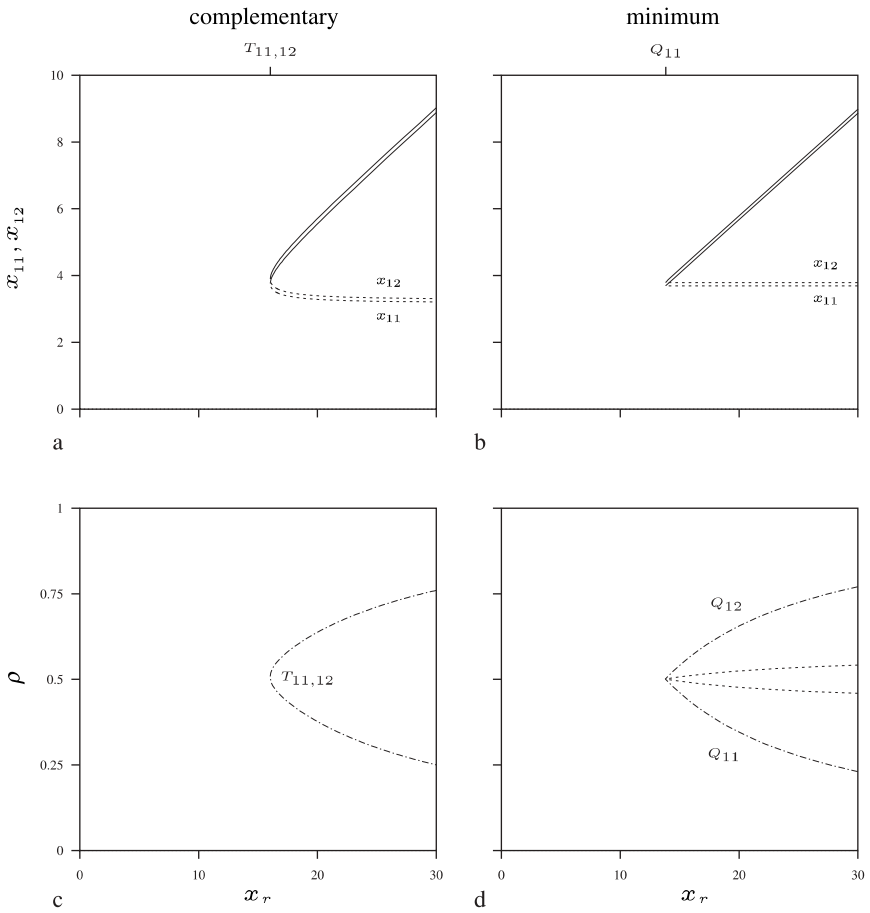

Fig. 4. Bifurcation diagrams with obligate symbiosis between two prey without the predator (Fig. 6(a)): One-parameter diagrams for complementary (**a**) and minimum (**b**) symbiosis for equilibrium values of the prey x_{11} and x_{12}. The bifurcation parameter is the concentration in the reservoir is x_r where $\rho = 0.5$. The dilution rate is $D = 0.1$. Two-parameter bifurcation diagrams for minimum (**c**) and complementary (**d**) symbiosis where the bifurcation parameters are the concentration in the reservoir is x_r and the mixing factor ρ. The dilution rate is $D = 0.1$.

products of the first prey population. Hence, roughly speaking, when the biomasses are below the saddle equilibrium values the system will collapse to extinction [40].

For obligate symbiosis with minimum symbiosis, close to $\rho = 0.5$ a codim-2 point serves as an organizing center. In the region bounded by the two curves Q_{11} and Q_{12} the two partner prey populations coexist. More precise, there is one stable and one unstable positive equilibrium. These curves are similar to the tangent bifurcation. In both cases a stable and unstable equilibrium coincide and disappear varying the free parameter. We will call this bifurcation a *pseudo-tangent* bifurcation. At the curve Q_{11} we have $x_{01}^*/(k_{01,11} + x_{01}^*) = p_{12}^*/(k_{12,11} + p_{12}^*)$, see

(14) where the star '*' denotes the equilibrium value for the single positive equilibrium. This curve is a kind of tangent bifurcation, since above this curve there is no positive equilibrium and directly below this curve there is one unstable, where for both prey populations the product of the partner prey is limiting, and one stable equilibrium, where for prey x_{11} nutrient x_{01} is limiting and for prey x_{12} the product of the partner prey p_{11} is limiting. Similarly, at the curve Q_{12} the following equality holds $x^*_{02}/(k_{02,12} + x^*_{02}) = p^*_{11}/(k_{11,12} + p^*_{11})$. Now just above this curve for prey x_{12} nutrient x_{02} is limiting and for prey x_{11} the product of the partner prey p_{12}. For the unstable equilibrium for both prey populations the product of the partner prey is limiting and this holds for the entire region between the curves Q_{11} and Q_{12}. In the region bounded by the two dashed curves in the positive stable equilibrium both essential nutrients are limiting for both prey populations.

In [28, 29] we derived the invasion criterion for a top-predator and a competitor prey population in a bi-trophic nutrient–prey food chain. For facultative symbiosis, invasion is via a transcritical bifurcation and the results can be derived analytically following a procedure proposed by Smith and Waltman (1994). For obligate symbiosis, the trivial equilibrium point $E_{01,02}$ is stable for all bifurcation parameter values since the Jacobian matrix evaluated in this point has 6 eigenvalues all equal to $-D$. (Two are directly the result of our assumption that the excreted products leave the reactor with dilution rate D). We conclude that the prey populations can never invade the virgin system consisting of only nutrients.

4.1. Host-symbiont association

An example for a host-symbiont association is the symbiotic association between algae (symbiont) and other protoctists, plants or animals (host). The algae requires ammonia from the host for growth in addition to light as nutrient and the host requires carbohydrates from the algae for extra growth on top of that allowed by its food supply [31].

This symbiotic association of the two populations is a mixture of facultative and obligate symbiosis. We select for the host (plant) x_{11} consuming x_{01} and p_{12} supplementary, and for the symbiont (fungi or algae) x_{12} consuming its resources x_{02} and p_{11}, complementary.

We show in Fig. 5 a one-parameter and a two parameter diagram for a host-symbiont association. When both trophic interactions are supplementary, there are two transcritical bifurcations, namely TC_{11} where the prey x_{11} can invade the nutrient system in equilibrium $E_{01,02}$ and $TC_{11,12}$ where the prey x_{12} can invade the nutrient–prey system in equilibrium E_{11}. For ρ-values close to 1 the two-parameter diagram resembles the diagram Fig. 3(b,d) while for ρ-values close to 0 it resembles Fig. 4(a,c). No tangent bifurcation is present. As a consequence there is no bi-stability of one stable interior equilibrium and one stable zero equilibrium.

5. Bifurcation analysis of the model with predation

We describe the two-parameter bifurcation diagrams for the whole food web, thus including the predator. First, in order to have a reference case, we analyse the food

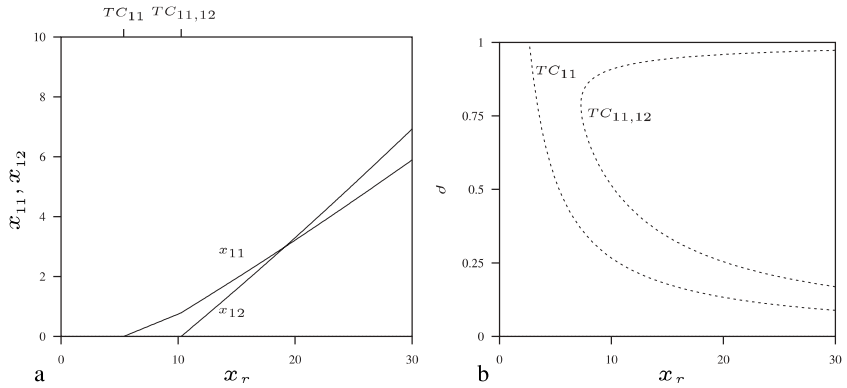

Fig. 5. Bifurcation diagrams with mixed symbiosis between two prey without the predator. One-parameter diagram (**a**) for equilibrium values of the prey x_{11} and x_{12}. The bifurcation parameter is the concentration in the reservoir is x_r where $\rho = 0.5$. The dilution rate is $D = 0.1$. Two-parameter bifurcation diagram (**b**) where the bifurcation parameters are the concentration in the reservoir is x_r and the mixing factor ρ. The dilution rate is again $D = 0.1$.

web without symbiosis. Second, we extend this model with facultative symbiosis where the products of the partner prey population are non-essential. Third, we study obligate symbiosis where the products of the partner prey population are essential.

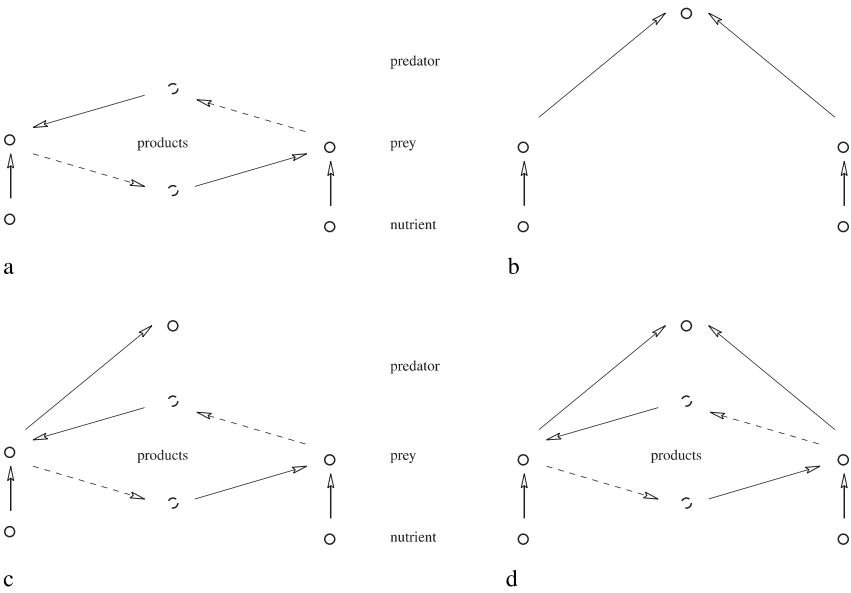

Fig. 6. Material flows through the food web with various interaction structures. **a** nutrient-prey-partner: **b** generalist predator without symbiotic association between prey species: **c** specialist predator: **d** generalist predator.

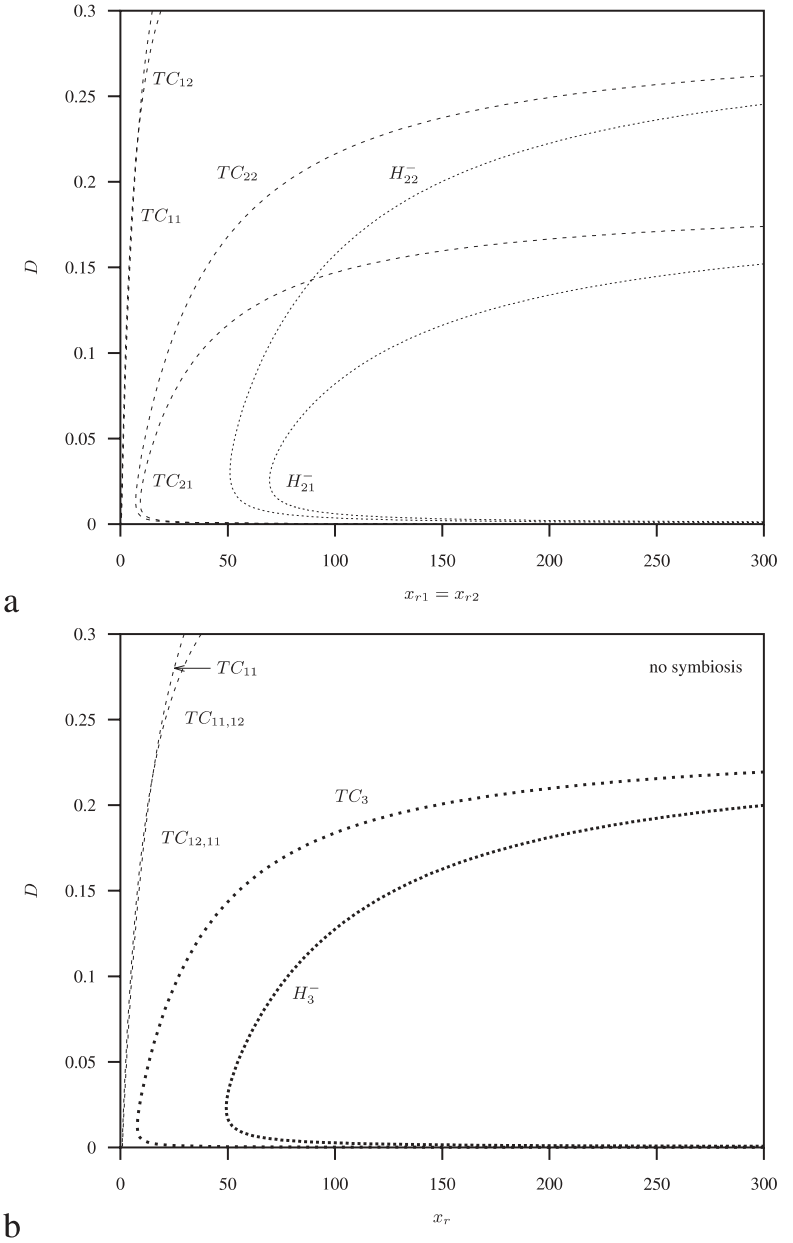

Fig. 7. Bifurcation diagram (**a**) for both nutrient–prey–predator systems separately. Bifurcation parameters are the dilution rate D and the substrate concentration in reservoir, x_{r1} and x_{r2}. Values assigned to physiological parameters and reference values for the perturbation parameters are listed in Table 3. Curves TC_{21}, TC_{22} are transcritical bifurcation curves and H_{21}^-, H_{22}^- mark Hopf bifurcation curves. Bifurcation diagram (**b**) for food web without symbiosis via products (Fig. 6(b)). The sum of nutrient concentrations in the inflow x_r where $\rho = 0.5$, acts now as bifurcation parameter. Curve TC_3 is transcritical bifurcation curve and H_3^- marks a Hopf bifurcation curve for the food web.

5.1. No symbiosis

The trophic interactions for this food web structure are shown in Fig. 6(b). In Fig. 7(a) we show a superposition of two bifurcation diagrams, namely one for the bi-trophic food chain where $x_{11} = 0$ and the other where $x_{12} = 0$, calculated with model (5). The curves TC_{21} and TC_{22} are transcritical bifurcation curves and H_{21}^- and H_{22}^- mark Hopf bifurcation curves.

The biologically important regions for the x_{01},x_{11},x_2 system are:

- left to TC_{11}: stable equilibrium E_{01} of nutrient system
- right to TC_{11} and left to TC_{21}: stable equilibrium $\mathrm{E}_{01,11}$ of nutrient-prey system
- right to TC_{21} and left to H_{21}^-: stable interior equilibrium, $\mathrm{E}_{01,11,2}$
- right to H_{21}^-: stable interior limit cycle, $\mathrm{L}_{01,11,2}$

Hence, the sequence of attractors that occur in order by increasing the parameter x_r while D is fixed, is:

$$\mathrm{E}_{01} \xrightarrow{TC_{11}} \mathrm{E}_{01,11} \xrightarrow{TC_{21}} \mathrm{E}_{01,11,2} \xrightarrow{H_{21}^-} \mathrm{L}_{01,11,2} \,. \tag{16}$$

The same holds for the x_{02},x_{12},x_2 system. Since the maximum growth rate of the predator x_2 consuming prey x_{12}, $\mu_{12,2} = 0.3$, is larger than consuming prey x_{11}, $\mu_{11,2} = 0.2$, curves TC_{22} and H_{22}^- lie on the left-hand side of TC_{21} and H_{21}^-, respectively.

Figure 7(b) gives the bifurcation diagram of the model without symbiosis where the predator consumes the substitutable prey population (see Fig. 6(b)). The attractors (Table 4), that occur in order by increasing the parameter x_r, where the fixed dilution rate $D = 0.1$, are:

$$\mathrm{E}_{01,02} \xrightarrow{TC_{12}} \mathrm{E}_{12} \xrightarrow{TC_{12,11}} \mathrm{E}_{11,12} \xrightarrow{TC_3} \mathrm{E}_{11,12,2} \xrightarrow{H_3^-} \mathrm{L}_{11,12,2} \,. \tag{17}$$

The two important bifurcation curves are the transcritical, TC_3 and the Hopf, H_3^-, bifurcation curves. This result indicates an inhibitory effect of the less "efficient" prey for the predator feeding on the two prey population. When $x_{12} = 0$, that is the predator consumes x_{11} only, the region where the predator can invade is larger but with $x_{11} = 0$ this region is smaller than when the predator consumes both substitutable prey population simultaneously.

5.2. Specialist predator

In Fig. 6(c) the trophic interactions for the food web structure, where the predator x_2 consumes one prey x_{11}, are shown. We will only consider the complementary symbiosis case for the two prey populations. Figure 8(a) gives the two-parameter diagrams for various maximum growth rates of the predator, Fig. 8(a) $\mu_{11,2} = 0.2$ (the reference value given in Table 3), (b) $\mu_{11,2} = 0.3$, (c) $\mu_{11,2} = 0.4$ and (d) $\mu_{11,2} = 0.45$. The maximum ingestion rate $I_{11,2}$ is changed accordingly, so that the efficiency remains constant $y_{11,2} = \mu_{11,2}/I_{11,2} = 0.6$. When $\mu_{11,2} = 0.2$ the diagram is similar to the standard one for a food chain without symbiosis Fig. 7(b),

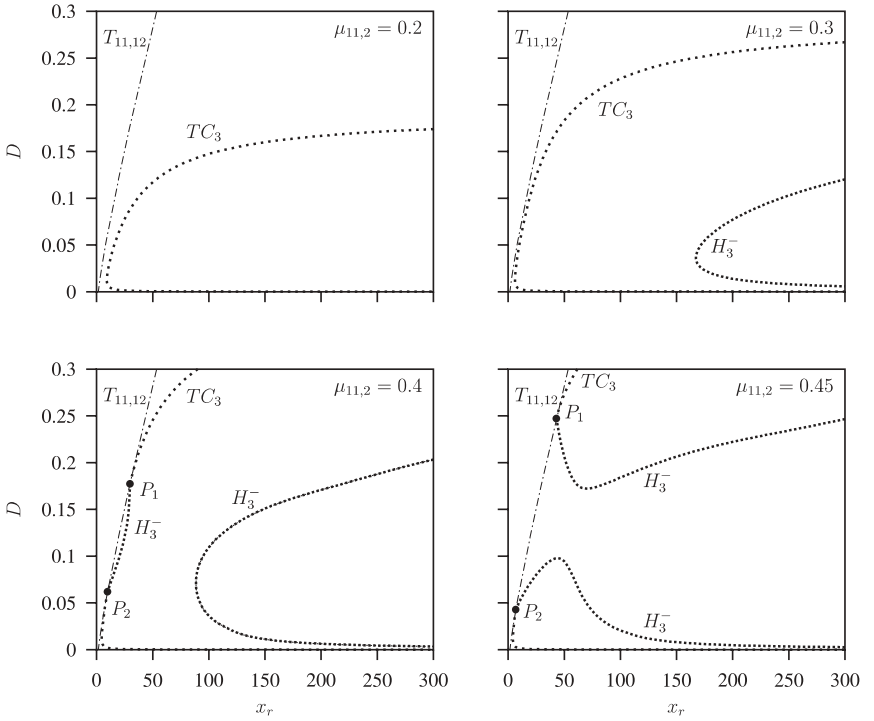

Fig. 8. Bifurcation diagram for food web for obligate complementary symbiosis via products with various maximum growth rates of the specialist predator (Fig. 6(c)). Bifurcation parameters are the dilution rate D and the sum of the nutrient concentrations in the inflow x_r, where $\rho = 0.5$. Curve $T_{11,12}$ is the tangent bifurcation curve where on the right-hand side both prey populations coexist in absence of the predator. Curve TC_3 is the transcritical bifurcation curve for $\mu_{11,2} = 0.2$ (**a**), $\mu_{11,2} = 0.3$ (**b**), $\mu_{11,2} = 0.4$ (**c**) and $\mu_{11,2} = 0.45$ (**d**).

except for the tangent bifurcation $T_{11,12}$ which replaces the transcritical bifurcations TC_{11}, TC_{12}, $TC_{12,11}$ and $TC_{11,12}$.

For the six-dimensional system without predator, one equilibrium in the positive cone of $\mathbb{R}^6$ is unstable and denoted by $\mathrm{E}^+_{11,12}$ and the other denoted by $\mathrm{E}^-_{11,12}$ is stable, while the zero equilibrium $\mathrm{E}_{01,02}$ is also stable. With the introduction of a predator, the unstable one $\mathrm{E}^+_{11,12}$ remains unstable, but now in $\mathbb{R}^7$, with still one real eigenvalue being positive. The equilibrium $\mathrm{E}^-_{11,12}$ becomes, however, unstable in $\mathbb{R}^7$ in points on the right-hand side of the transcritical bifurcation TC_3 in the two-parameter bifurcation diagram. There is one real positive eigenvalue and therefore the point is a saddle. Finally the zero equilibrium $\mathrm{E}_{01,02}$ remains stable in $\mathbb{R}^7$. The stable manifold of the saddle is the separatrix between the multiple attractors. On the right-hand side of $T_{11,12}$, a transcritical bifurcation TC_3 marks the region where the predator can coexist with the prey populations. The predator can invade via the equilibrium, $E^-_{11,12}$.

Increasing the maximum growth rate enlarges the region where it can invade, that is, the curve TC_3 moves to the left. However, for instance when $\mu_{11,2} = 0.3$,

there is a Hopf bifurcation curve H_3^- for the x_r range we study. The interior equilibrium in the positive cone of $\mathbb{R}^7$, with positive predator biomass $E_{11,12,2}$, is stable above the Hopf bifurcation curve H_3^-, and is an unstable focus below this curve. On the right-hand side of this Hopf bifurcation curve there is coexistence on a limit cycle.

For $\mu_{11,2} = 0.4$ the transcritical bifurcation curve TC_3 intersects the tangent bifurcation curve $T_{11,12}$ twice in the zero-pair codim-2 points denoted by P_1 and P_2. In these points one eigenvalue and the real part of two conjugate eigenvalues are zero. Observe that these codim-2 points are degenerate and the bifurcation diagram near these points differ from those in the generic codim-2 fold-Hopf case (see [34]). Between these points the transcritical bifurcation is now on the unstable branch (points $E_{11,12}^+$) originating from the tangent bifurcation curve $T_{11,12}$ (see Fig. 4(c)). This part of the curve TC_3 is not shown in the diagrams. Invasion via the stable branch (points $E_{11,12}^-$) is now always possible via the tangent bifurcation points $T_{11,12}$ between the points P_1 and P_2. Simulations show that the solution after invasion via points $E_{11,12}^-$ close to the curve $T_{11,12}$ always converges to the stable zero solution $E_{01,02}$, that is, all biota go extinct.

A "new" Hopf bifurcation curve connects these points P. The other Hopf bifurcation H_3^- similar to the one present for $\mu_{11,2} = 0.3$, envelopes a large region of the parameter space shown in Fig. 8.

Increasing the maximum growth rate further, see the diagram where $\mu_{11,2} = 0.45$, shows that the two "vertical" branches of the Hopf bifurcation curve merge and break simultaneously in the "horizontal" direction so that two separated branches emanate now in the codim-2 points P. At the transition point where the two branches switch connection, as in a Hopf bifurcation point, there are two complex conjugate eigenvalues with real part equal to zero.

The curves in the bifurcation diagrams do not give the complete picture of the long-term dynamics dependence on the bifurcation parameters. For, close to the right-hand side of the tangent curve $T_{11,12}$ invasion of a predator does not lead to a positive attractor and close to the Hopf bifurcations H_3^- curves, there is, a positive attractor. Hence there must be another bifurcation curve which separates the two regions in the bifurcation diagram where on one side the zero biomass solution is the only attractor and where on the other side a positive attractor exists. We will return to this subject in the next section.

5.3. Generalist predator

The trophic interactions for this food web structure are shown in Fig. 6(d). We will discuss subsequently facultative symbiosis and obligatory symbiosis for this food web connection pattern.

5.3.1. Facultative symbiosis

The bifurcation diagram for the whole food web where the prey populations consume their essential nutrient and the product produced by the partner prey is show in Fig. 9. The sequence of attractors that occur in order by increasing the parameter x_r is essentially the same as in (17).

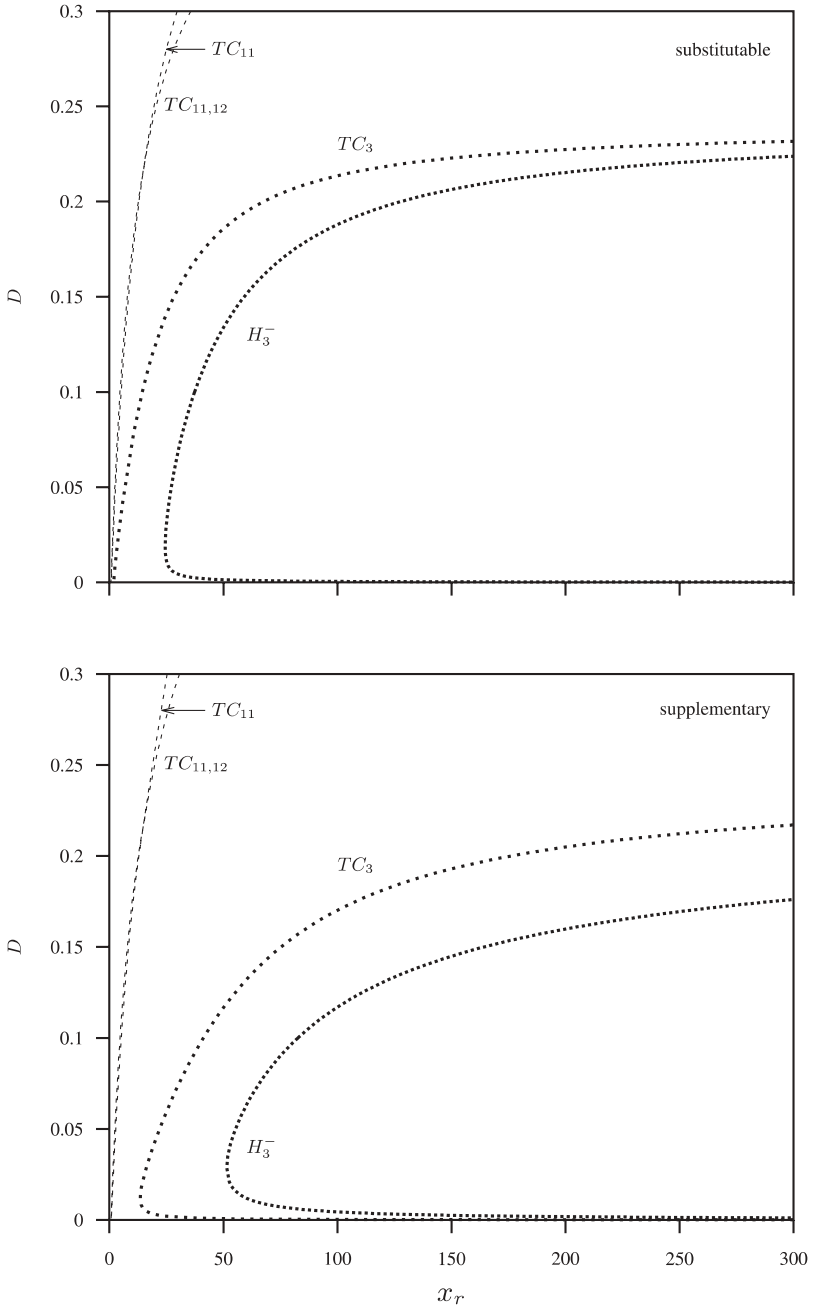

Fig. 9. Bifurcation diagram for food web for facultative substitutable (**a**) and supplementary (**b**) symbiosis via products (Fig. 6(d)). The bifurcation parameters are the dilution rate D and the sum of the equal nutrient concentrations in the inflow x_r, where $\rho = 0.5$. The curve TC_3 is the transcritical bifurcation curve. The curve $TC_{11,12}$ is the transcritical bifurcation curve where prey population x_{12} can invade the two-nutrient–one-prey system.

Figure 10 shows the biomass densities where D is varied for a fixed nutrient inflow $x_r = 30$ and $\rho = 0.5$. For this nutrient input in the complementary case oscillatory behaviour occurs in the mid-range values for the dilution rate. The minimum biomass densities for the two prey populations (not shown in Fig. 10) become very small already just above the Hopf bifurcation point H_3^-. This indicates that stochastic fluctuations would lead to extension of the prey population and therefore the predator population as well. This holds for a large portion of the two parameter diagrams shown in Fig. 9. Therefore, it is safe to state that persistence occurs only in the regions between the transcritical and the Hopf bifurcations.

5.3.2. Obligatory symbiosis

In Fig. 11 the diagrams for the food web with obligatory symbiosis between the prey populations are depicted. The products of the partner prey are complementary to the nutrients or each prey population is limited by only one resource at a time. These diagrams differ much from those for the facultative symbiosis cases presented in Fig. 9.

Complementary symbiosis Observe that for large D values in Fig. 11(a) there is a tangent bifurcation when no predator is present. This bifurcation is denoted by $T_{11,12}$. This curve goes through two zero-pair codim-2 points P_1 and P_2 where two eigenvalues are zero. These points lie on a tangent bifurcation curve $T_{11,12}$ and a transcritical bifurcation curve TC_3 while a Hopf bifurcation curves H_3^- originate in these points.

The sequence of attractors that occur in order by increasing the parameter x_r for D-values between P_1 and P_2 is simple, that is for the whole range only the zero-state is the single attractor. Hence, none of the two prey populations can invade via a transcritical bifurcation.

The sequence of attractors that occur in order by increasing the parameter x_r for D-values above P_1 differs also substantially from that described earlier

$$\mathrm{E}_{01,02} \xrightarrow{T_{11,12}} \mathrm{E}_{11,12} \xrightarrow{TC_3} \mathrm{E}_{11,12,2} \xrightarrow{H_3^-} \mathrm{L}_{11,12,2} \xrightarrow{G_e^{\neq}} \mathrm{E}_{01,02}\,. \tag{18}$$

At the left-hand side of the transcritical bifurcation curve TC_3 the predator cannot invade, but on the right-hand side it can. This stable interior equilibrium becomes unstable at the Hopf bifurcation H_3^- where a stable limit cycle $L_{11,12,2}$ emanates.

What happens changing D with the limit cycle $L_{11,12,2}$ is now explained. To that end we fix x_r. Figure 12 shows the biomass densities where D is varied for a fixed nutrient inflow $x_r = 30$ and $\rho = 0.5$ for the complementary Fig. 12(a) and minimum Fig. 12(b) symbiosis cases. Below the top branch Hopf bifurcation there is a heteroclinic cycle which connects the two non-zero saddle (one eigenvalue is positive) equilibria $\mathrm{E}_{11,12}^-$ and $\mathrm{E}_{11,12}^+$ where the predator is absent.

Lowering D the period of the stable limit cycle increases rapidly. The minimum of the predator becomes low during a large portion of the limit cycle. This is clear from Fig. 13(a) where the unstable limit cycle is shown in the x_{11}, x_{12}, x_2 space. Starting with a small x_2 value close to the saddle equilibrium $\mathrm{E}_{11,12}^-$, which is stable when the predator is absent, the predator biomass increases. It "passes" the unstable

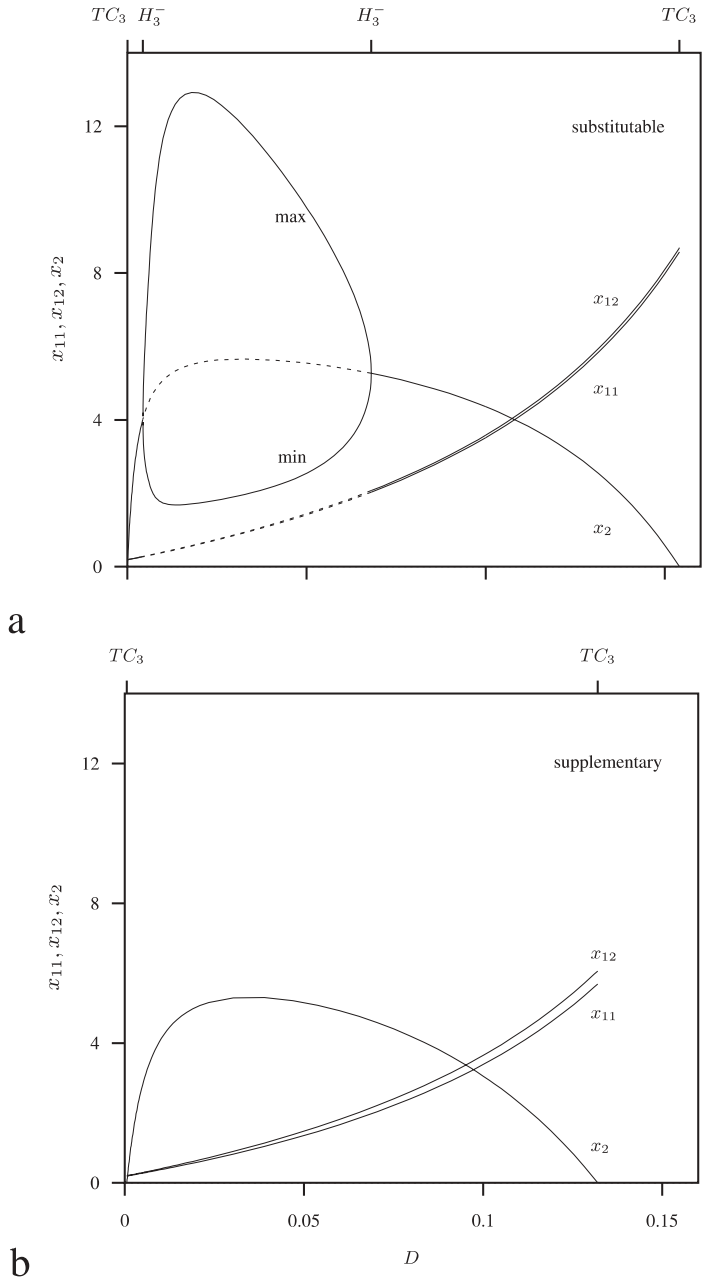

Fig. 10. One-parameter bifurcation diagram for food web for facultative substitutable (**a**) and supplementary **b** symbiosis between two prey with the predator. Equilibrium and extremes values of the prey x_{11}, x_{12} and predator x_2 are plotted. Bifurcation parameter is the dilution rate D. The concentration in the reservoir is fixed by $x_r = 30$ and $\rho = 0.5$. Solid curves denote stable equilibrium and extreme values and dashed curves unstable equilibrium values.

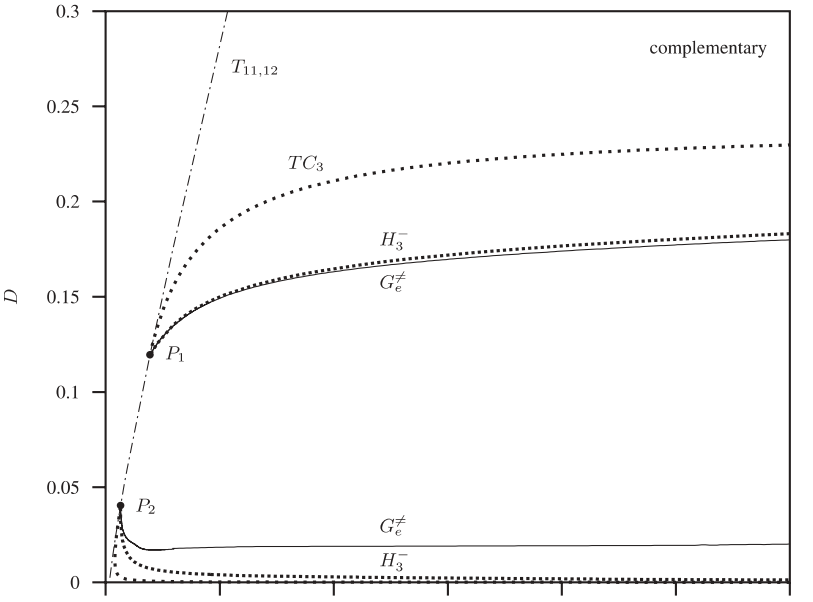

a

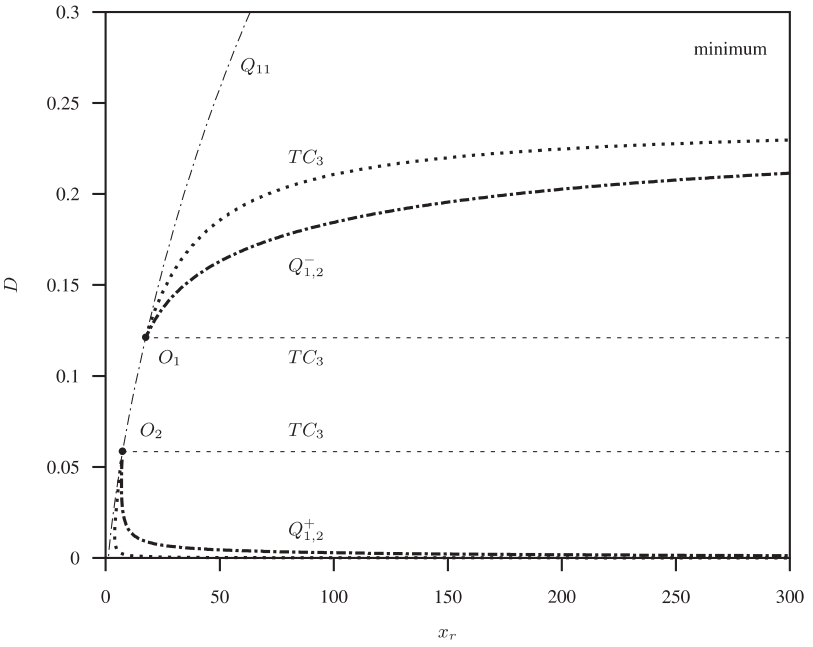

b

Fig. 11. Bifurcation diagram for food web for obligate symbiosis via products (Fig. 6(d)). Complementary (**a**) and minimum (**b**) symbiosis. Bifurcation parameters are the dilution rate D and the sum of the nutrient concentrations in the inflow x_r, where $\rho = 0.5$. Curve TC_3 is the transcritical bifurcation curve. Curve $T_{11,12}$ is the tangent bifurcation curve where on the right-hand side both prey populations coexist.

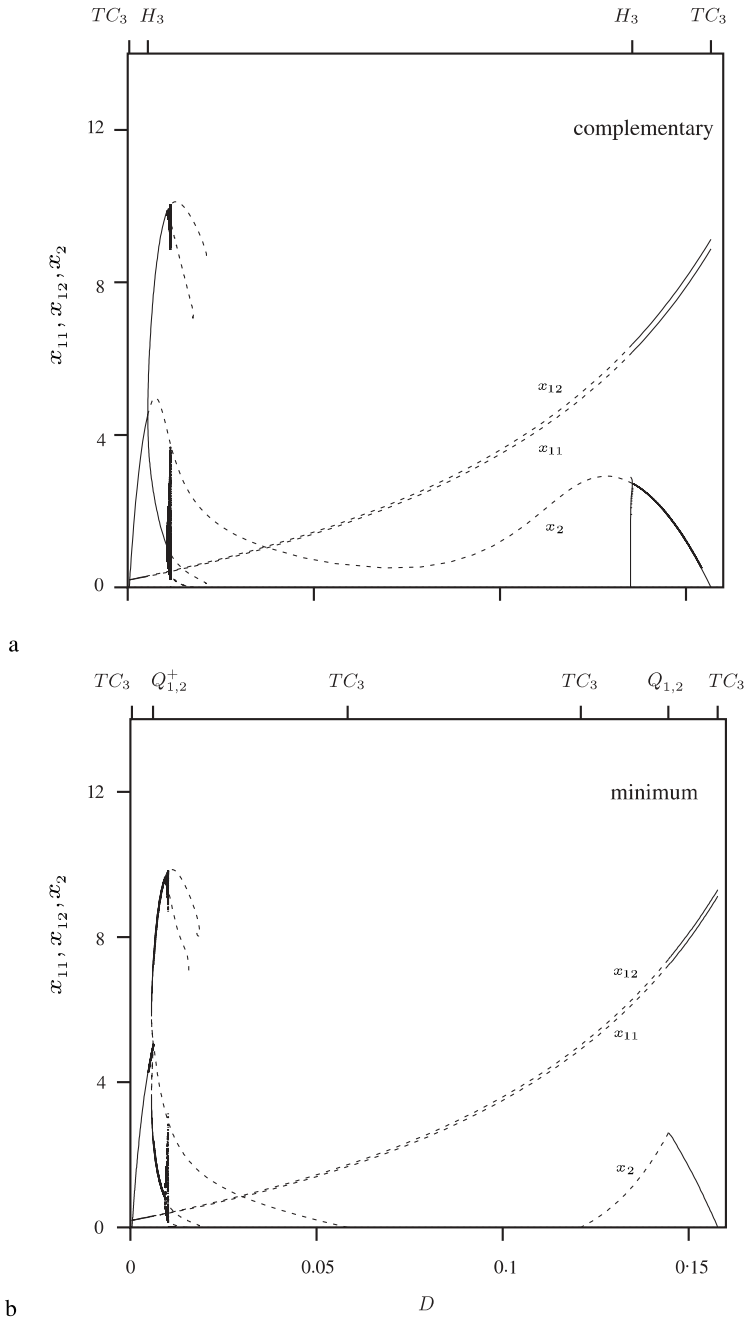

Fig. 12. One-parameter bifurcation diagram for food web with obligate complementary (**a**) and minimum (**b**) symbiosis between two prey with the predator. Equilibrium and extremes values of the prey x_{11}, x_{12} and predator x_2. Bifurcation parameter is the dilution rate is D. The concentration in the reservoir is fixed by $x_r = 30$ and $\rho = 0.5$. Solid curves give stable equilibrium values. Dashed curves give unstable equilibrium values.

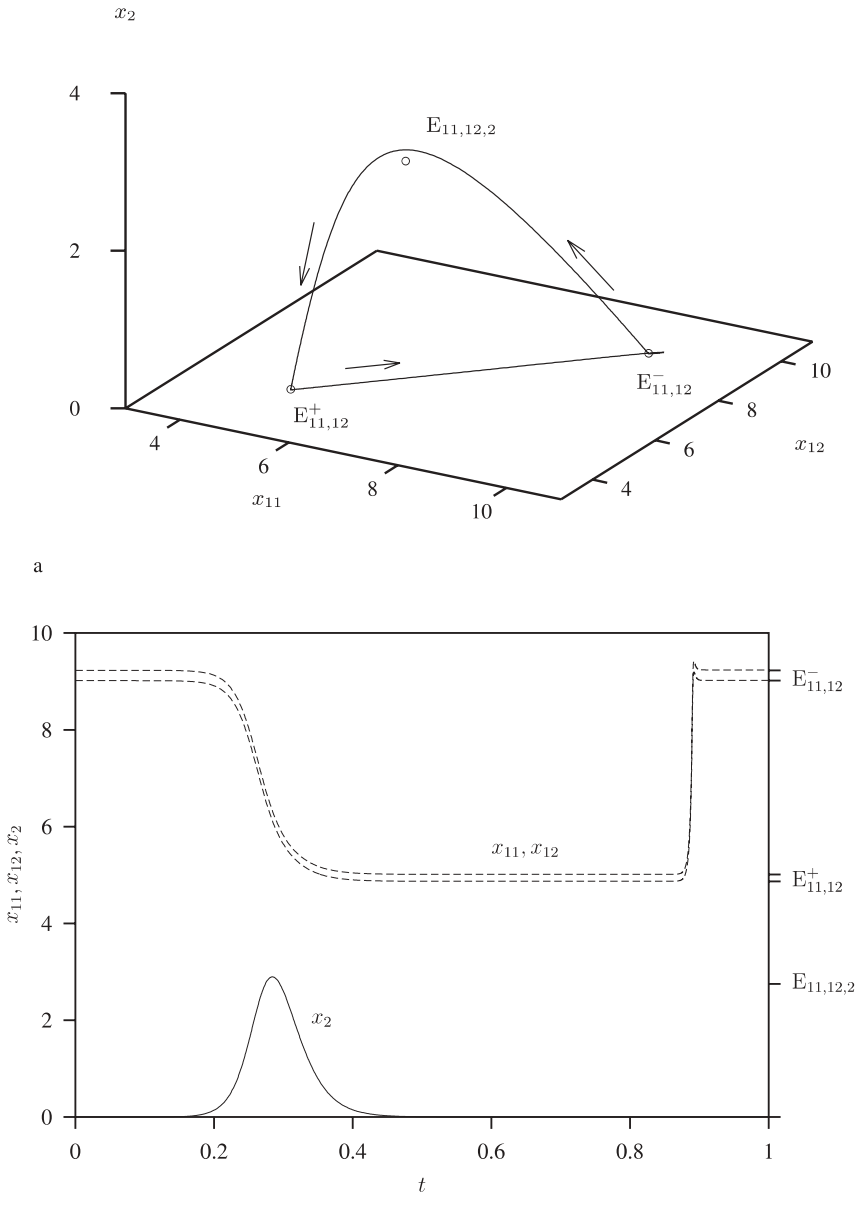

Fig. 13. Heteroclinic loop of the complementary symbiosis case plotted in the x_{11}, x_{12}, x_2 space which connects two unstable equilibria in the zero-predator plane (**a**). Time evolution plot (**b**) shows $x_{11}(t)$, $x_{12}(t)$ and $x_2(t)$. The concentration in the reservoir is $x_r = 30$ and the mixing factor $\rho = 0.5$ and the dilution rate is the critical value at $G_e^{\neq}$.

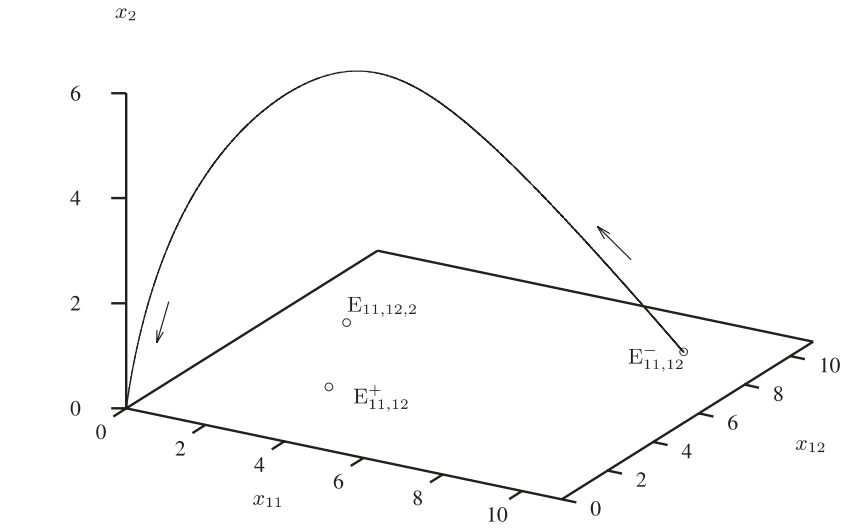

a

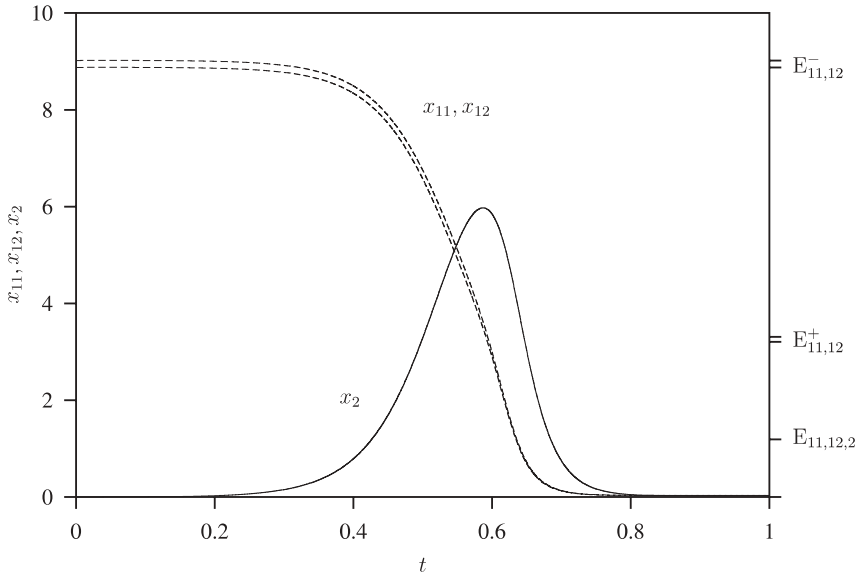

b

Fig. 14. Orbit (**a**) in the complementary symbiosis case with initial point is at $E^{-}_{11,12}$ where $x_2 = 0.001$ and the orbit terminates at $E_{01,02}$ where only the two nutrients are in the reactor. Time evolution plot (**b**) shows the biomass densities $x_{11}(t), x_{12}(t)$ and $x_2(t)$. The dilution rate $D = 0.1$, concentration in the reservoir $x_r = 30$ and mixing factor $\rho = 0.5$.

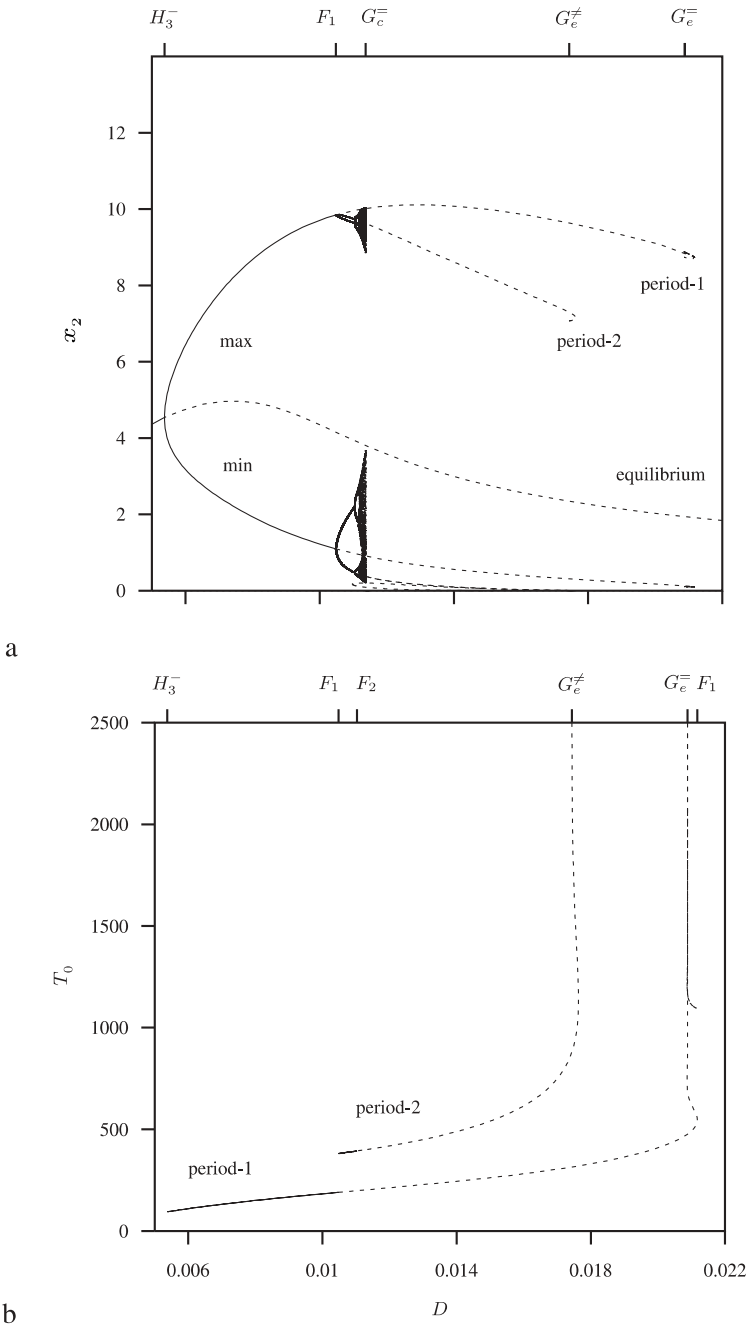

Fig. 15. Detail of one-parameter bifurcation diagram Fig. 12(a) for food web with complementary symbiosis between two prey with the predator where chaos occurs. In figure **a** the predator biomass density x_2 and in figure **b** the period T_0 are plotted as function of the the dilution rate D.

interior equilibrium $E_{11,12,2}$ and finally the predator biomass decreases and the orbit approaches the equilibrium $E^{+}_{11,12}$, which is unstable when the predator is absent. Now, the biomass of the predator is almost zero and the orbit continues close to the zero-predator invariant plane where $x_2 = 0$ toward the the point where it started. In Fig. 13(b) the biomasses are plotted as a function of the scaled time. These result show the long episodes in the neighbourhood of the two saddle points.

Lowering D further, breaks this limit cycle at a global heteroclinic bifurcation (it cannot be deduced from local information at this point) $G^{\neq}_{e}$. The predator, when introduced in small amounts, does not eventually settle itself together with the prey populations. In Fig. 14 the biomasses are plotted as function of time for $D = 0.1$ and $x_r = 30$. The initial point is close to the stable equilibrium $E^{-}_{11,12}$ of the six dimensional two-nutrients–two-products–two-prey system which is a saddle equilibrium for the seven dimensional two-nutrients–two-products–two-prey–predator system and therefore the predator can invade. After invasion, however, the prey biomasses become low after which the predator goes extinct as well.

More complicated phenomenon occur for dilution rates below point P_2. Now we increase D starting from a stable interior equilibrium. In Fig. 15(a) which is a detail of Fig. 12(a), the biomass of the predator population x_2 are plotted as a function of D. Above the lower branch Hopf bifurcation curve H^{-}_{3}, increasing D gives a cascade of period doubling leads to chaotic dynamics. The first period doubling, at the flip bifurcation point, is indicated by F_1.

Following the period-1 limit cycle, it approaches a homoclinic Shil'nikov bifurcation. The interested reader is referred to [27,35] for the description of this homoclinic bifurcation of the equilibrium of a tri-trophic food chain. In Fig. 15(b) the period of the limit cycle as function of the dilution rate D is depicted. Approaching the Shil'nikov bifurcation point, the period approached infinity. The orbit of the system stays a relatively long episode close to the unstable equilibrium followed by a large excursion through the state space.

Following the period-2 limit cycle, which originates at the flip bifurcation F_1, reveals that this cycle becomes unstable itself at the flip bifurcation F_2, where the period-4 cycle originates. Thereafter, the minimum biomass density x_2 approaches zero at the global bifurcation $G^{\neq}_{e}$, the heteroclinic connection. Similar to the Shil'nikov bifurcation point, here also the period approached infinity. Now the period-2 orbit stays for relatively long episodes close to the two saddle points as shown in Fig. 13.

For a D value just above the F_1 point the chaotic attractor disappears abruptly at a global bifurcation denoted by $G^{=}_{c}$. Figure 16 shows a detail of one-parameter bifurcation diagram Fig. 15. Careful inspection shows that the minimum points cluster at the boundary of three chaotic bands. This suggest the existence of a boundary crisis [45,26] for a period-3 unstable limit cycle. Therefore we study a Poincaré next-return map.

For this seven-dimensional continuous-time system a Poincaré next-return map P to a particular two-dimensional plane, namely where the predator x_2 has a minimum, is constructed. In Fig. 17 a projection of the first and third iterate of Poincaré map P are plotted. To a very good approximation all points appear to lie on a single curve, the graph of an invertible two-value function (such as the Hénon map). At

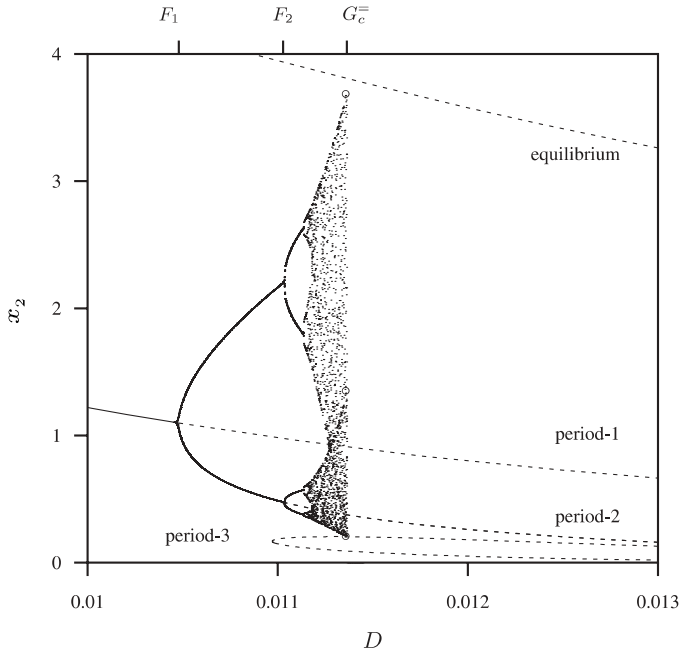

Fig. 16. Details of one-parameter bifurcation diagram Fig. 15 for food web with complementary symbiosis between two prey with the predator where chaos occurs. The minimum value of the biomass density x_2 is plotted as function of D where $x_r = 30$.

the critical D value the chaotic attractor disappears abruptly. These points are associated with so called crises where a chaotic attractor disappears (boundary crises) or changes shape (interior crises) abruptly together with the basin of attraction, see also [26].

The third iterate graph in Fig. 17 suggests that the period-3 orbit exhibits a homoclinic tangency at the critical D value. In Fig. 16 the minimum values for this period-3 limit cycle is also plotted as a function of D. This plot shows that the chaotic attractor is cut by the unstable branch of the period-3 limit cycle in a boundary crisis. The D value marks a homoclinic bifurcation for a period-3 limit cycle denoted by $G_c^=$, see [6]. We refer to [6, 7, 26] for a description of the dynamics around this type of global bifurcation.

We conclude that for $x_r = 30$, above the global bifurcation curve $G_c^=$ the zero equilibrium $E_{01,02}$ is global attracting, see Fig. 14, except for higher period stable curves, for instance close to the Shil'nikov bifurcation.

This complex bifurcation structure suggests that the unfolding in the codim-2 point P_2 differs from that of P_1. Since, for higher values of D the stable limit cycle originating at the upper branch of the Hopf bifurcation curve H_3^- with increasing amplitude leads directly to the heteroclinic connection, while at the lower branch with smaller D values there are global bifurcations, at least for the period-1, period-2 and period-3 orbits.

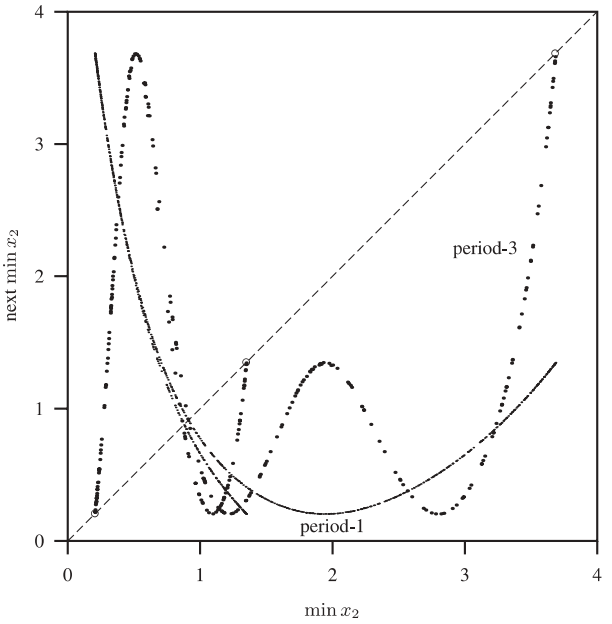

Fig. 17. Next minimum and third iterate of Poincaré map for minimum value of the biomass density of the predator x_2 at the global bifurcation denoted by $G_c^=$ where critical values $D = 0.0113571$ and $x_r = 30$.

Figure 18 is a detail of Fig. 11(a) in the region of the parameter space close to point P_2. Continuation of the flip bifurcation curve F_1 reveals that it intersects the global bifurcation curve $G_e^{\neq}$ and this clarifies why for $x_r = 30$ the heteroclinic connection occurs as a limiting situation for the period-2 orbit. We conclude that close to the point P_2 there is no flip bifurcation and no chaotic behaviour and the bifurcation patterns around the points P_1 and P_2 are similar.

Continuation of the Shil'nikov bifurcation gives a U-shaped curve also found in [27,35]. Hence, there is no codim-2 end-point for $x_r \approx 10$. The curve $G_e^=$ was continued starting at $x_r = 30$ with $T_0 = 2500$ fixed and D and x_r as bifurcation parameters. Coming back at $x_r = 30$, we do end at a D value that differs slightly from the D value of our stating point. Therefore, in Fig. 15 label $G_e^=$ indicates actually two points in the plots, indistinguishably close to each other. This point was used as a starting point for the continuation with D and T_0 as bifurcation parameters where $x_r = 30$ remained constant. The result is shown in Fig. 15(b). It is the period-2 curve visible on the left-hand side of the period-1 curve where the period T_0 increases rapidly (see also [27]). The period-2 curve is connected to the period-1 curve and hence also to the Hopf bifurcation point H_3^-.

Minimum symbiosis Figure 11(b) gives the diagram for the food web with minimum symbiosis. This diagram differs from the previous one for the complementary symbiosis case. There are two codim-2 points denoted by O_1 and O_2. These points are interactions of the transcritical bifurcation curve TC_3 and the pseudo-tangent

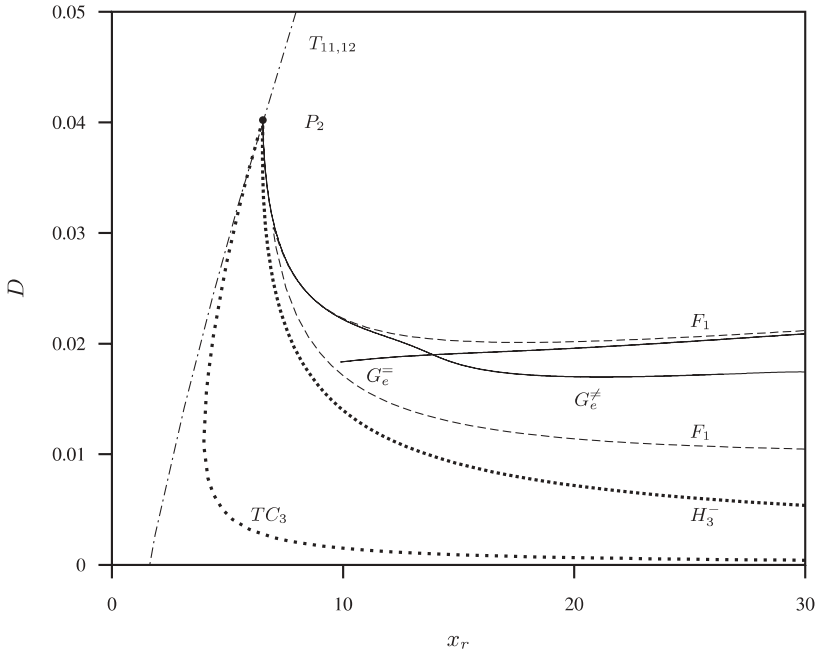

Fig. 18. Details of two-parameter bifurcation diagram Fig. 11 close to the codim-2 point P_2. Curve F_1 is a flip bifurcation curve, $G_e^=$ Shil'nikov bifurcation curve, $G_e^{\neq}$ heteroclinic bifurcation curve. The flip bifurcation curve and the heteroclinic bifurcation curve intersect.

bifurcation curve Q_{11} (see Fig. 4(d) with $\rho = 0.5$). From these points a pseudo-tangent bifurcation curve $Q_{1,2}^-$ and a pseudo-tangent bifurcation curve $Q_{1,2}^+$ originate, respectively. Notice that there are actually two curves, for there are two prey populations that switch most limiting nutrient. Hence, all four combinations are possible, for instance a state where prey x_{11} is growth limited by its nutrient x_{01} while prey x_{12} is growth limited by the products of its partner p_{11}. However, for the reference parameter values given in Table 3 both prey populations switch most limiting resources almost at the same time and the curves are indistinguishable in the diagrams. At the curve $Q_{1,2}^-$ the predator goes extinct catastrophically. In principle, varying the free parameter the system could converge to the two-prey population system $\mathrm{E}_{11,12}$ where the predator is absent, but simulation show that the solution converges to the trivial equilibrium $\mathrm{E}_{01,02}$, as in Fig. 14.

The sequence of attractors that occur in order by increasing the parameter x_r for D-values above O_1 and below O_2, differs from (18) for high x_r-values.

$$\mathrm{E}_{01,02} \xrightarrow{Q_{11}} \mathrm{E}_{11,12} \xrightarrow{TC_3} \mathrm{E}_{11,12,2} \xrightarrow{Q_{1,2}} \mathrm{E}_{11,12} \ . \tag{19}$$

The establishment of the two prey population for low nutrient supply, small x_r, is similar to the complementary symbiosis case described in the previous paragraph, the tangent bifurcation $T_{11,12}$ is replaced by the pseudo-tangent bifurcation Q_{11}.

Figures 12(b) and 19 give the one-parameter bifurcation diagram for the minimum symbiosis case, where $x_r = 30$. They are similar to those of the complementary symbiosis case shown in Fig. 12(a) and 15. The global bifurcations for the period-1, period-2 and period-3 will be similar too and therefore they are not discussed here. There is, however, a striking difference in the way the period-1 orbit emanates. For the complementary symbiosis case this happens at a Hopf bifurcation point. Here, below the curve $Q^-_{1,2}$ all populations die out after invasion of the predator. Comparison with Fig. 12(a) for the complementary symbiosis case suggest that the Hopf bifurcation curve H_3^- coincides with the heteroclinic bifurcation curve $G_e^{\neq}$.

Above the curve $Q^+_{1,2}$ there exists a stable limit cycle. This does not originate at a Hopf bifurcation point but at the point $Q^+_{1,2}$ where the most limiting nutrient of one of the prey population switches. We recall that for the parameter values we took ($\rho = 0.5$), with increasing D also the most limiting nutrient of the other prey switches, but both switches occur at almost the same D-value. We call the switch point with the lowest D value a pseudo-Hopf bifurcation $Q^+_{1,2}$. Crossing the curve $Q^+_{1,2}$ the Jacobian matrix is discontinuous with respect to parameter D. Below the curve $Q^+_{1,2}$ the real parts of the leading eigenvalues are negative giving the stable focus, but above this curve these parts are positive yielding the unstable focus. Thus, varying the parameter D these real parts jump over the imaginary axis. This is just as with the Hopf bifurcation, however now in a discontinuous fashion. As for a subcritical Hopf bifurcation, an unstable limit cycle emanates. Observe that on the limit cycle during one period there are switches of the most limiting nutrients both ways. Figure 12 (b) shows that the limit cycle becomes stable at a tangent bifurcation of this period-1 limit cycle.

The time solution for the mass densities of the nutrients and populations are shown in Fig. 20(a) starting close to $E^+_{11,12}$ and for parameter values $x_r = 30$, $\rho = 0.5$ and $D = 0.1$. The results are very similar to those for the complementary symbiosis case shown in Fig. 14. In the minimum symbiosis case at about $t = 170$ shortly after each other both products of the partners become most limiting. For comparison we calculated also the case where no switches of the most limiting resources occurs. In that case the solution depicted in Fig. 20(b) converges to a stable interior equilibrium. We conclude that before the first switch the system evolves towards the positive stable equilibrium where the nutrients determine the growth rate, but after both switches the products of the partners become most limiting and the solution converges to the zero biomass densities solution.

6. Discussion

The bifurcation diagrams Figures 3 and 4 for the four symmetric symbiotic interactions between two nutrient feeders need further explanation. With facultative symbiotic association between the two partners, the region of positive coexistence in the two-parameter diagram Fig. 3(c,d) is bounded by (supercritical) transcritical bifurcations. When the association is obligate this region is bounded by a tangent (complementary symbiosis) or a pseudo-tangent (minimum symbiosis) bifurcation (Fig. 4(c,d)).

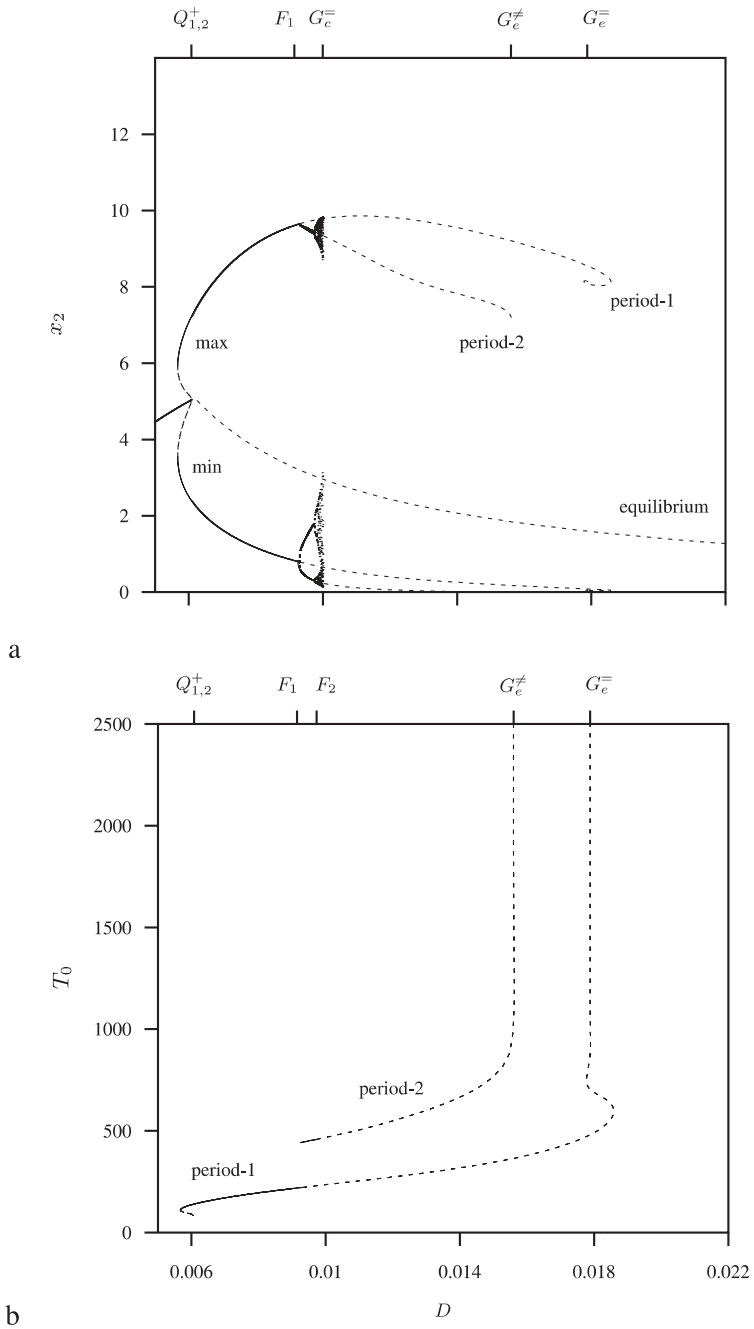

Fig. 19. Detail of one-parameter bifurcation diagram Fig. 12(b) for food web with minimum symbiosis between two prey with the predator where chaos occurs. In figure **a** the biomass density x_2 and in figure **b** the period T_0 are plotted as function of the the dilution rate D.

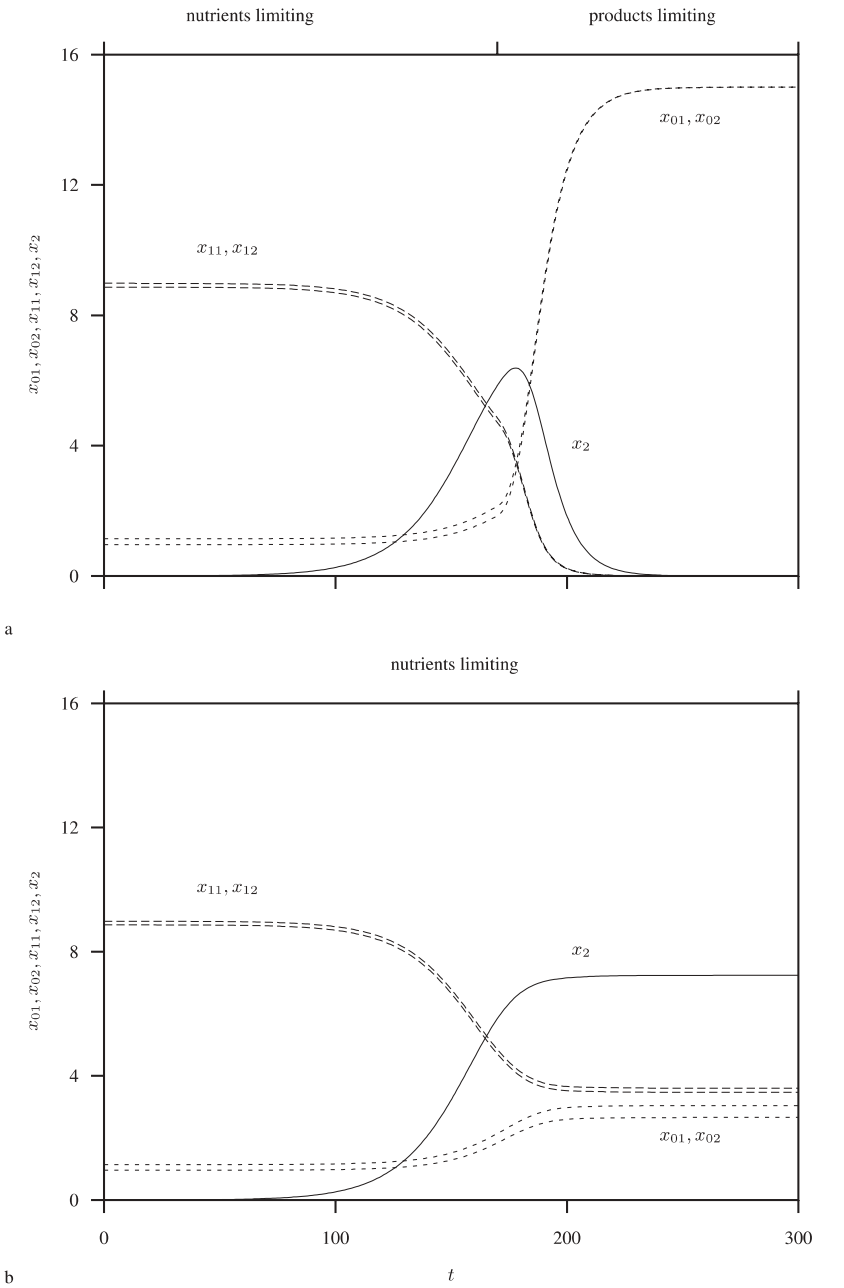

Fig. 20. Time evolution (**a**) of the biomass densities $x_{11}(t)$, $x_{12}(t)$ and $x_2(t)$ for minimum symbiosis (top). The dilution rate $D = 0.1$, concentration in the reservoir $x_r = 30$ and mixing factor $\rho = 0.5$. The initial point is close to $E^+_{11,12}$ where $x_2 = 0.001$ and the orbit terminates at $E_{01,02}$ where only the two nutrients remain in the reactor. For comparison the results are also presented (**b**) when no switch would occur, that is the nutrients are always the most limiting resources for the prey populations.

These bifurcation patterns express mathematically that a pair of facultative symbiotic nutrient feeders (prey populations) can invade the chemostat with only nutrients one by one when the nutrient supply is sufficiently large. With obligate symbiosis on the other hand invasion is only possible for sizeable cohorts of both partners and not as single individuals. Hence, for obligate mutualistic prey associations the food web can only be assembled from a bare region, when both populations enter that region at the same time with biomasses sufficiently large. When the biomasses are below the saddle equilibrium values the system will collapse towards extinction [40].

The result that two prey populations with obligate symbiosis cannot coexist as a result of invasion where both populations are initially rare is well known [47]. This fact is sometimes used as evidence for the greater abundance of obligate symbiosis in tropical environment. In [47] it is mentioned that obligate symbiosis are rather common in the temperate zone. However, in pioneer communities where populations necessarily start at low densities should by our model go to extinction.

These phenomena bear properties which resemble what occurs with a one-population Allee-effect model [1]. Also in that case the zero solution is always stable and separated by a saddle equilibrium from a positive stable equilibrium. Lewis and Kareiva (1993) and Owen and Lewis (2001) show that a population can colonize a bare country by spread during primary succession. This is similar to metapopulations with diffusion, where the average population density is below the critical values but in some patches sufficiently high to have persistence and later on a dispersal when food supply is sufficient [24].

Back to two symbiotic populations, succession of facultative and obligate symbiosis is possible. That is, the parameters, that fix the symbiotic relationship, change at an evolutionary time-scale so that initially symbiosis is facultative and it changes into an obligate relationship. Kooijman *et al.* (2003) propose a similar mechanism with the transition from two free-living interacting populations into a single fully integrated endosymbiotic one.

Competitive exclusion forbids coexistence of two populations feeding on the single resource. Two partner populations with substitutable symbiotic interaction can, however, coexist on a single nutrient ($\rho = 0$ or $\rho = 1$ in Fig. 3(c)). Figure 3(d) shows that supplementary symbiosis is not sufficient, hence for both populations their nutrient and the product of the partner have to be non-essential.

We selected substitutable and supplementary as examples for facultative symbiosis and complementary and minimum for obligate symbiosis. Other multiple resource functional responses are proposed in the literature. An example of a facultative multiple resource is the perfectly substitutable version [17,50] where the growth rate is just a linear combination of the two growth rates when the resources are consumed separately. This form, which we will call *additive*, is justified under special conditions when the two resources are ingested independently, that is specific carriers for each different resources are present and their assimilation into biomass is via multiple assimilation pathways. Additive multiple resources were used for predator–prey interactions in [19,31]. In these papers, microorganisms are modelled consisting of two components, representing structural biomass and

reserve material. The ratio of these components may vary and therefore these organisms form two resources for the predator.

The *multiplicative* version falls under the category of obligate associations where both functional responses on the separate resources are multiplied. In [23] the resources engaged in this type of multiple resource interaction were called interactively essential resources. This multiplicative version was used to model interactive effects between the resources on growth of competing species feeding on multiple resources. In [31] this type of functional response is derived with classical time-budget theory. In contrast to the minimum formulation, it is possible to derive this version starting with a pseudo-reaction scheme. It is, however, argued that this version is biologically not realistic, [31]. In Table 2 the growth rates for all symbiotic associations are summarized.

Generally, with the Liebig minimum law formulations the minimum is taken of the specific growth rates of the population when it would consume each resource solely. Here we take the minimum of the scaled functional responses and the resulting minimum value is multiplied by a single maximum growth rate for the population irrespective of which resource is most limiting. This formulation was also used in [18]. Our motivation is that it makes a better comparison possible with the complementary resources formulation. Observe that with multiplicative resources there is also one maximum growth rate parameter associated with the consumer. The ingestion rate for each resource is derived from the growth rate by multiplication with a constant factor that is the amount of the resource contained in a unit of population (see [17]).

The facultative versions have two maximum growth parameters for each prey population, namely for prey x_{11}: $\mu_{01,11}$ and $\mu_{02,11}$ and they occur in the two terms that describe the growth rate $\mathcal{M}$ defined in (15c). In the literature the obligate versions (minimum or multiplicative) have always a single growth term and as a consequence only one maximum growth parameter which we denoted by $\mu_{01,11}$, [17]. On the contrary, with our mass-balance model formulation we used the two term formulation because it shows that also in these versions two resources contribute to the total resource consumption. Thus, the multiplicative version has also an additive aspect when mass fluxes are concerned. It is important that the maximum growth rates occurring in these two terms are equal, for there is one single process rate that determines the two resource consumption rates and the growth rates as well.

In our mass-balance formulation the starting point is the ingestion rate and therefore the scaled functional responses are multiplied by the maximum ingestion rates for the trophic interaction formulation, (15a) and (15b). The growth rate results after the resources are processed in the assimilation process, maintenance process and growth process, (15). Therefore, the actual maximum growth rate depends on the yield and maintenance rate coefficient besides the maximum ingestion rate. In our model formulation the maximum (abundant food and maintenance zero) growth rate parameter $\mu_{ij,kl}$ is essentially the maximum ingestion rate divided by the yield, that is $\mu_{ij,kl} = I_{ij,kl}/y_{ij,kl}$. As a consequence the diagrams of Fig. 2 can be compared with those given in the literature [17,50].

The diagrams in Fig. 9 for facultative symbiosis are similar to the one given in Fig. 7(b). When no predator is present we found on the right-hand side of the bifurcation curves $TC_{11,12}$ always a stable bounded and positive equilibrium as in the weak interaction facultative mutualism case, [33]. This is in contrast to the classical Lotka-Volterra type model for the strong interaction facultative mutualism case where mutualism has a destabilizing effect.

When this system is extended by a predator consuming the prey populations the bifurcation diagrams can be much more complicated and we stress that other bifurcations than shown in the diagrams are possible.

When the trophic interaction between the predator and the two prey populations is weak there is stable coexistence in a large part of the bifurcation diagram. For larger maximum ingestion and growth rates of the predator, unstable positive equilibria exists, just as with the bi-trophic nutrient–prey–predator food chain for large nutrient concentrations in the inflow. The region with stable equilibrium persistence is, however, larger than without symbiosis. Obviously, the substitutable and supplementary products appear to be stabilizers for the whole food web. This finding is in agreement with the results reported in [47] for a four species food web where a Lotka-Volterra model was used in simulation studies taking parameter values randomly.

For obligate symbiosis the situation differs a lot. A tangent bifurcation marks the region where the two prey populations can live together. There is a stable as well as an unstable positive equilibrium in addition to the stable zero equilibrium. The predator can invade via the stable positive branch when the dilution rate is not too large, see Fig. 11. When the predator is a generalist, the food web can persist as a positive stable equilibrium in only a small region of the parameter space. We conclude that complementary and minimum symbiosis has a destabilizing effect due to over-exploitation when the growth rate of the predator is large but with moderate maximum growth rates it has a stabilizing effect similar as in the case of the specialist predator (see diagrams Fig. 8 for $\mu_{11,2} = 0.2$ and $\mu_{11,2} = 0.45$).

The model with minimum symbiosis is more difficult to analyse than the complementary symbiosis case. With the Liebig minimum law the Jacobian matrix is discontinuous with respect to a parameter when another nutrient becomes the most limiting nutrient. We called these points also bifurcation points since the long-term dynamic behaviours changes quantitatively. The repertoire of these changes, however, is much more diverse than the classical variant of bifurcation point which are derived by a normal form analysis. What happens after the switch has to be determined by taking all resources one by one the most limiting resource and this gives the clue to which situation the solution goes after crossing the bifurcation point. The dynamic behaviour in time is however always well defined. The right-hand sides of the ODEs satisfy the Lipschitz condition with respect to the state variables (see also [38]). Hence, we have uniqueness of the initial value problem.

As in the classical Lotka-Volterra type model for obligatory mutualism the zero solution is always stable. For low nutrient input x_r it is the sole equilibrium as in the Lotka-Volterra model for weak interaction obligatory mutualism, [33]. When the nutrient input x_r is higher there is, as in the Lotka-Volterra model for strong

interaction obligatory mutualism, a positive unstable equilibrium. however, in the mass-balance formulation there is a bounded positive stable equilibrium while in the Lotka-Volterra type model there is not.

In [2] a three dimensional ODE model for a two aged forest affected by insect pest is investigated. They found that a stable limit cycle disappears via a heteroclinic bifurcation, that is, invasion of a small number of pests into a steady-state forest system could lead to a complete degradation of the system similar to that occurring in the two cases with obligatory symbiosis.

A simple two-dimensional predator–prey model with Allee effect analysed in [3] shows also a similar global bifurcation. In many classical predator–prey models a logistic growth (a polynomial of degree two in the prey populations biomass) describes the temporal change of the prey biomass. In order to model Allee effect this polynomial is replaced by a polynomial of degree three

$$\frac{dx_1}{dt} = x_1(x_1 - l)(1 - x_1) - x_1x_2 \ , \tag{20a}$$

$$\frac{dx_2}{dt} = (x_1 - m)x_2 \ , \tag{20b}$$

where l and m are compound parameters (see [3]). The predator consumes the prey with a simple linear functional response like in a Lotka-Volterra predator-prey system. There are three equilibria without predation, two stable (one is the zero equilibrium) and one unstable in between. With predation these points lie in the coordinate plane of the positive quadrant. The zero stable equilibrium remains stable but the other becomes unstable, a saddle equilibrium. The additional interior equilibrium becomes unstable in a Hopf bifurcation where a stable limit cycle originates. Varying a bifurcation parameter yields oscillatory behaviour which becomes severe so that the stable limit cycle visits the two positive saddle equilibria with zero predator. Finally it breaks open at a global bifurcation a heteroclinic cycle, a connection between the two saddles. Changing the parameter beyond this point both populations die out and cannot re-establish themselves since this zero equilibrium is stable.

Bazykin studied also a one-predator–two-preys system where the dynamics of the preys without predation is described by (1) and the predator consumes both preys with a linear Lotka-Volterra functional response as in (20). Similar global bifurcation are reported, and even a heteroclinic connection composed of three orbits connecting three saddle points.

For a specialist predator, from the two codim-2 points P_1 and P_2 in Fig. 8 heteroclinic bifurcation curves, $G_e^{\neq}$, emanate as in Fig. 11 for the generalist predator. However, in the middle range between the two points, the global bifurcation turns into a homoclinic bifurcation curve to a saddle. A description of all local and global bifurcations for this case is beyond the scope of this paper.

In [15] the dynamics of a population of residents that is being invaded by an initially rare mutant is studied. The observed bifurcation patterns that make overexploitation possible, are similar to those associated with “evolutionary suicide”. These phenomena are related to “attractor switching” in systems with multiple

attractors. In [15] it is shown that attractor switching is possible near a bifurcation point where the resident attractor undergoes a discontinuous change. Such bifurcations are called catastrophic and with food chains and food webs we found subcritical transcritical [28], tangent (saddle-node) [28,48,12], subcritical Hopf, subcritical flip [27] bifurcations for equilibria and limit cycles. Near a supercritical transcritical bifurcation, invasion leads to settlement of the invader together with the populations that were already present. Generally, in food chain models invasion via a subcritical transcritical bifurcation, leads also to settlement of the invader or in food web models replacement of a competitor [30]. However, in the case of over-exploitation the invaded population goes eventually extinct. With obligatory symbiosis, direct attractor switching is illustrated in Fig. 20 for the minimum symbiosis case. With complementary symbiosis such a switch is not clear from Fig. 20. In both cases in the region in the parameter space of interest, invasion has a destabilizing effect since the limit solution after invasion is a stable limit cycle. Breaking of this stable limit cycle at the global bifurcation point results in an abrupt disappearance of the basin of attraction of the interior limit cycle and consequently with parameter variation the zero stable equilibrium becomes attracting after invasion.

7. Conclusions

Two prey populations with substitutable symbiosis can co-exist on a single nutrient. The partner is not a predator but coprophagic, it does not consume the prey itself but its products. We conclude that a single nutrient can support in addition to food chains where each populations is consumed by at most one other population, food webs with more complicated trophic interactions.

For the reference value of the maximum growth rate of a specialist predator feeding on one prey population (Table 3), there is a stable equilibrium coexistence in a large region of the control parameter space. Increasing the maximum growth rate leads to an enlargement of this region where the predator can invade, but over-exploitation gives extinction in a large part of this region. So, the region with stable equilibrium is effectively smaller. As a result a higher maximum growth rate is not advantageous with respect to persistence of the food web.

When the predator is a generalist, for the parameter values given in Table 3 in a large region of the bifurcation diagram, over-exploitation leads to the destruction of the food web, while stable coexistence of both partners without predator is possible. Comparison of the bifurcation diagrams in Fig. 8 and 11 suggests that increasing the growth rate (and therefore invasibility) by addition of another food source has more effect than increasing the maximum growth rate of a single resource with respect to the generation of oscillations or even over-exploitation.

The difference in the dynamics behaviour for the facultative and obligate symbiosis is striking and is robust for changes of the intrinsic species parameters and of those describing the trophic interactions. For facultative symbiosis, invasion of the prey populations is smooth via a transcritical bifurcation while for obligate symbiosis a tangent bifurcation is involved. This implies bi-stability where one equilibrium is the zero-prey's state.

The effect of over-exploitation by the predator on the obligate prey symbiosis is interesting from an evolutionary point of view. When the maximum growth rate is taken as the fitness measure to be optimized that enhances invasibility a large maximum growth rate can be counter-productive. Such a predator can invade, but soon it will exhaust its prey and goes extinct as well.

Comparison of Figures 14 and 20 shows that results obtained for the minimum model can be used to interpret those of the complementary model. Obviously in the complementary model the prey populations are initially limited in growth most by the nutrients while eventually the products of the partners are most limiting.

The mass-balance formulation treats symbioses which involve interactions that influence resource supply, in the same way as competition and predation. This makes it possible to integrate the study of symbiosis in the context of food web analysis, as stated as one of the future tasks for ecology in [21].

Acknowledgements. We would like to thank Martin Boer for valuable discussions and Marcel van der Heijden for comments on the manuscript.

References

1. Allee, W.C.: Cooperation among Animals, with Human Implications. New York: Henry Schuman, 1951
2. Antonovsky, M.Y., Fleming, R.A., Kuznetsov, Y.A., Clark, W.C.: Forest–pest interaction dynamics: The simplest mathematical models. Theor. Population Biol. **37**, 343–367 (1990)
3. Bazykin, A.D.: Nonlinear dynamics of interacting populations. Singapore: World Scientific, 1998
4. Begon, M., Harper, J.L., Townsend, C.R.: Essentials of Ecology. Oxford: Blackwell Science, 2000
5. Boer, M.P.: The dynamics of tritrophic food chains. Ph.D. thesis, Vrije Universiteit, de Boelelaan 1087, 1081 HV Amsterdam, The Netherlands, 2000
6. Boer, M.P., Kooi, B.W., Kooijman, S.A.L.M.: Homoclinic and heteroclinic orbits in a tri-trophic food chain. J. Math. Biol. **39**, 19–38 (1999)
7. Boer, M.P., Kooi, B.W., Kooijman, S.A.L.M.: Multiple attractors and boundary crises in a tri-trophic food chain. Math. Biosci. **169**, 109–128 (2001)
8. Boucher, D.H.: The Biology of Mutualism: Ecology and Evolution. New York: Oxford University Press, 1985
9. Boucher, D.H., James, S., Keeler, K.H.: The ecology of mutualism. Annu Rev. Eco. Syst. **13**, 315–347 (1982)
10. Bronstein, J.L.: Our current understanding of mutualism. Quarterly Rev. Biol. **69**, 31–43 (1994)
11. Cunningham, A., Nisbet, R.M.: Transients and oscillations in continuous culture. In: Mathematics in Microbiology (M.J. Bazin, ed.), London: Academic Press, 1983, pp. 77–103
12. De Roos, A.M., Persson, L.: Size-dependent life-history traits promote catastrophic collapses of top predators. Proc. Nat. Acad. Sci. USA **99**, 12907–12912 (2002)
13. Doedel, E.J., Champneys, A.R., Fairgrieve, T.F., Kuznetsov, Y.A., Sandstede, B., Wang, X.: AUTO 97: Continuation and Bifurcation software for ordinary differential equations. Technical report, Concordia University, Montreal, Canada, 1997
14. Edelstein-Keshet, L.: Mathematical Models in Biology. Random House, 1988

15. Geritz, S.A.H., Gyllenberg, M., Jacobs, F.J.A., Parvinen, K.: Invasion dynamics and attractor inheritance. J. Math. Biol. **44**, 548–560 (2002)
16. Golubski, A.J.: Potential impacts of multiple partners on Mycorrhizal community dynamics. Theor. Population Biol. **62**, 47–62 (2002)
17. Grover, J.P.: Resource Competition. Population and Community Biology series. London: Chapman & Hall, 1997
18. Grover, J.P.: Stoichiometry, herbivory and competition for nutrients: Simple models based on planktonic ecosystems. J. Theor. Biol. **214**, 599–618 (2002)
19. Hanegraaf, P.P.F., Kooi, B.W., Kooijman, S.A.L.M.: The role of intracellular components in food chain dynamics. Comptes rendus de lAcademie des science series III Sciences de la vie life **323**, 99–111 (2000)
20. Hernandez, M.J., Barradas, I.: Variation in the outcome of population interactions: bifurcation and catastrophes. J. Math. Biol. **46**, 571–594 (2003)
21. Hoeksema, J.D., Bruna, E.M.: Pursuing the big questions about interspecific mutualism: a review of theoretical approaches. Oecologia **125**, 321–330 (2000)
22. Huisman, J., Weissing, F.J.: Biodiversity of plankton by species oscillations and chaos. Nature **402**, 407–410 (1999)
23. Huisman, J., Weissing, F.J.: Oscillations and chaos generated by competition for interactively essential resources. Ecological Res. **17**, 175–181 (2002)
24. Hutsin, V., Law, R., Lewis, D.: Dynamics of ecologically obligate mutualism: Effects of spatial diffusion on resilience of the interacting species. Am. Naturalist **126**, 445–449 (1985)
25. Khibnik, A.I., Kuznetsov, Y.A., Levitin, V.V., Nikolaev, E.V.: Continuation techniques and interactive software for bifurcation analysis of ODEs and iterated maps. Physica D **62**, 360–371 (1993)
26. Kooi, B.W., Boer, M.P.: Chaotic behaviour of a predator-prey system. Dynamics of Continuous Discrete and Impulsive Systems Series B Applications and Algorithms **10**, 259–272 (2003)
27. Kooi, B.W., Boer, M.P., Kooijman, S.A.L.M.: Consequences of population models on the dynamics of food chains. Math. Biosci. **153**, 99–124 (1998)
28. Kooi, B.W., Boer, M.P., Kooijman, S.A.L.M.: Resistance of a food chain to invasion by a top predator. Math. Biosci. **157**, 217–236 (1999)
29. Kooi, B.W., Kooijman, S.A.L.M.: Invading species can stabilize simple trophic systems. Ecological Modelling **133**, 57–72 (2000)
30. Kooi, B.W., Kuijper, L.D.J., Boer, M.P., Kooijman, S.A.L.M.: Numerical bifurcation analysis of a tri-trophic food web with omnivory. Math. Biosci. **177**, 201–228 (2002)
31. Kooijman, S.A.L.M.: Dynamic Energy and Mass Budgets in Biological Systems. Cambridge: Cambridge University Press, 2000
32. Kooijman, S.A.L.M., Auger, P., Poggiale, J.C., Kooi, B.W.: Quantitative steps in symbiogenesis and the evolution of homeostasis. Biol. Rev. **78**, 435–463 (2003)
33. Kot, M.: Elements of Mathematical Ecology. Cambridge: Cambridge University Press, 2001
34. Kuznetsov, Y.A.: Elements of Applied Bifurcation Theory, volume 112 of Applied Mathematical Sciences. New York: Springer-Verlag, 2 edition, 1998
35. Kuznetsov, Y.A., De Feo, O., Rinaldi, S.: Belyakov homoclinic bifurcations in a tritrophic food chain model. SIAM J. Appl. Math. **62**, 462–487 (2001)
36. Kuznetsov, Y.A., Levitin, V.V.: CONTENT: Integrated environment for the analysis of dynamical systems. Centrum voor Wiskunde en Informatica (CWI), Kruislaan 413, 1098 SJ Amsterdam, The Netherlands, 1.5 edition, 1997
37. Lewis, M.A., Kareiva, P.: Allee dynamics and the spread of invading organisms. Theor. Population Biol. **43**, 141–158 (1993)

38. Li, B., Smith, H.L.: How many species can two essential resources support? SIAM J. Appl. Math. **62**, 336–366 (2001)
39. May, R.M.: Stability and Complexity in Model Ecosystems. New Haven: Princeton University Press, 1973
40. May, R.M.: Theoretical Ecology: Principles and Applications. Sunderland: Sinauer Associates, 1981
41. Metz, J.A.J., Diekmann, O.: The dynamics of physiologically structured populations, volume 68 of Lecture Notes in Biomathematics. Berlin: Springer-Verlag, 1986
42. Morin, P.J.: Community Ecology. Blackwell Science, 1999
43. Murray, J.D.: Mathematical Biology, volume 19 of Biomathematics Text. Springer-Verlag, 1989
44. Odum, E.P.: Fundamentals of Ecology. Philadelphia: W. B. Saunders Co., 1963
45. Ott, E.: Chaos in Dynamical Systems. Cambridge: Cambridge University Press, 1993
46. Owen, M.R., Lewis, M.A.: How predator can slow, stop or reverse a prey invasion. Bulletin of Math. Biol. **63**, 655–684 (2001)
47. Ringel, M.S., Hu, H.H., Anderson, G.: The stability and persistence of mutualism embedded in community interactions. Theor. Population Biol. **50**, 281–297 (1996)
48. Scheffer, M., Carpenter, S., Foley, J.A., Folke C., Walker B.: Catastrophic shifts in ecosystems. Nature **413**, 591–596 (2001)
49. Smith, H.L., Waltman, P.: The Theory of the Chemostat. Cambridge: Cambridge University Press, 1994
50. Tilman, D.: Resource competition and community structure. Princeton: Princeton University Press, 1982
51. van der Heijden, M.G.A., Sanders I.R.: Mycorrhizal Ecology, volume 157 of Ecological Studies. Heidelberg: Springer-Verlag, 2002
52. Vandermeer, J., Boucher, D.H.: Varieties of mutualistic interaction in population models. J. Theor. Biol. **74**, 549–558 (1978)